NASA TECHNICAL NOTE

NASA TN D-3440

LOAN COPY: R
AFWL (W
KIRTLAND AFI

0130385

TECH LIBRARY KAFB, NM

NASA TN D-3440

QUASI-SLENDER BODY THEORY FOR SLOWLY OSCILLATING BODIES OF REVOLUTION IN SUPERSONIC FLOW

by Max F. Platzer and Gilbert H. Hoffman

George C. Marshall Space Flight Center
Huntsville, Ala.

NATIONAL AERONAUTICS AND SPACE ADMINISTRATION • WASHINGTON, D. C. • JUNE 1966

TECH LIBRARY KAFB, NM
0130385

QUASI-SLENDER BODY THEORY FOR SLOWLY OSCILLATING BODIES OF REVOLUTION IN SUPERSONIC FLOW

By Max F. Platzer and Gilbert H. Hoffman

George C. Marshall Space Flight Center
Huntsville, Ala.

NATIONAL AERONAUTICS AND SPACE ADMINISTRATION

For sale by the Clearinghouse for Federal Scientific and Technical Information
Springfield, Virginia 22151 – Price $3.00

TABLE OF CONTENTS

LIST OF ILLUSTRATIONS

LIST OF ILLUSTRATIONS (Cont'd)

LIST OF SYMBOLS

Symbol	Definition
a	center of rotation of body
c^*	free stream sound speed (dimensional)
C_N	normal force coefficient = $\frac{\text{normal force}}{q^*_\infty \; Q^*(\ell^*)}$
C_M	pitching moment coefficient = $\frac{\text{pitching moment}}{q^*_\infty \; Q^*(\ell^*)\; \ell^*}$
C_{N_α}, C_{M_α}	stability derivatives due to angle of attack
$C_{N_{\dot\alpha}} + C_{N_q}$	stability derivatives for total damping
$C_{M_{\dot\alpha}} + C_{M_q}$	in pitch
C_{N_δ}, C_{M_δ}	in-phase flutter derivatives
$C_{N_{\dot\delta}}$, $C_{M_{\dot\delta}}$	out-of-phase flutter derivatives
C_p	pressure coefficient = $\frac{p^* - p^*_\infty}{q^*_\infty}$
C_{p_1}	in-phase pressure coefficient
	derivative = $\frac{1}{\cos\theta}\left(\frac{\partial C_p}{\partial \delta}\right)_{\delta \to 0}$
C_{p_2}	out-of-phase pressure coefficient
	derivative = $\frac{1}{\cos\theta}\left(\frac{\partial C_p}{\partial \dot\delta}\right)_{\dot\delta \to 0}$
$F(x)$	doublet distribution

LIST OF SYMBOLS (Cont'd)

Symbol	Definition
k	reduced frequency = $\frac{\omega^* \ell^*}{U^*}$
ℓ^*	body length (dimensional)
M	free stream Mach number = $\frac{U^*}{c^*}$
$Q(x)$	body cross-sectional area = $\pi R^2(x)$
q^*_∞	free-stream dynamic pressure (dimensional)
$R(x)$	body radius
t	time measured in a body-fixed reference frame = $\frac{t^* \ell^*}{U^*}$
U^*	free-stream speed (dimensional)
u,v,w	velocity components in x, r, θ directions
$W(x)$	body center-line motion function defined by Eq. (34)
x,r,θ	body-fixed cylindrical coordinates (see Figure 1)
β	$\sqrt{M^2 - 1}$
$\delta(t)$	instantaneous angle of pitch
δ_0	amplitude of angle of pitch
ϵ	body fineness ratio = $R(1)$
κ	$\frac{k M}{\beta^2}$
ξ	dipole coordinate
λ	cross-flow out-of-phase perturbation potential
ψ	cross-flow in-phase perturbation potential

LIST OF SYMBOLS (Concluded)

Symbol	Definition
μ	$\frac{k\,M^2}{\beta^2}$
ρ	$\sqrt{(x-\xi)^2 - \beta^2 r^2}$
τ	time measured in a wind-fixed reference frame $= \frac{\tau^* \ell^*}{U^*}$
Φ	complex time - dependent perturbation potential
$\hat{\phi}$	complex perturbation potential defined by Eq. (20)
ϕ	axial-flow perturbation potential
χ	reduced complex perturbation potential defined by Eq. (32)
Ω	complete time - dependent velocity potential
ω^*	frequency of oscillation (dimensional)

SUBSCRIPTS AND SUPERSCRIPTS

$( )', ( )'',$ etc.	derivatives with respect to the independent variable
$( )_{x,r,\theta,t,\tau}$	partial derivatives
$( )^{(1)}$	first-order quantity
$( )^{(2)}$	second-order quantity
$\dot{( )}$	derivative with respect to time
$( )_R$	real part
$( )_I$	imaginary part

QUASI-SLENDER BODY THEORY FOR SLOWLY OSCILLATING BODIES OF REVOLUTION IN SUPERSONIC FLOW

SUMMARY

An analysis is presented which accounts for body shape and Mach number dependence of the aerodynamic forces on slowly oscillating pointed bodies of revolution in supersonic flow. By using body-fixed coordinates, the first order velocity potential is expanded in an elementary fashion for small radial distances from the body. This expansion is equivalent to the Adams-Sears expansion technique using Laplace or Fourier transforms. Analytical closed-form expressions for the stability derivatives are obtained. These results are valid to second-order in terms of Mach number and body thickness ratio.

Three specific body shapes are analyzed in detail: a cone, a convex parabolic ogive, and a concave parabolic ogive. Numerical results for the four stability derivatives C_{N_α}, C_{M_α}, $C_{N_{\dot{\alpha}}} + C_{N_q}$, and $C_{M_{\dot{\alpha}}} + C_{M_q}$ are presented to illustrate their dependence on Mach number and body thickness ratio. Comparisons with other theories are given, and the range of validity of the present results is discussed. Comments on application of quasi-slender-body theory to other body shapes are made.

INTRODUCTION

For the calculation of static and dynamic stability characteristics of large rocket vehicles in the high dynamic pressure portion of the ascent, which is usually the low supersonic flow regime, there exists a need for an easy-to-apply theoretical method that will show explicitly the effects of Mach number and body geometry. Munk's well-known slender-body concept [1] and its generalization to unsteady flow [2] are often found to be too inaccurate. Consequently, in recent years many investigators have tried to develop more accurate methods by either seeking a solution to the full linearized potential equation [3-11] or by attempting to solve the nonlinear equation [12-16].

Extensions of the Karman-Moore method [17] to the case of slowly oscillating bodies of revolution are given in References 8, 9 and 10. A similar extension of the Oswatitsch-Erdmann procedure [18] is proposed in Reference 11. References 12, 13 and 16 consider linearized time-dependent perturbations about the nonlinear axisymmetric flow. The resulting equations are then solved by the

method of characteristics. All of these approaches lead to purely numerical procedures and require a substantial amount of preparatory work.

A quite different nonlinear approach was developed by Revell [14] which is an extension of Lighthill's second-order slender-body theory [19] to slowly oscillating bodies of revolution. This method makes possible the determination of analytical closed-form expressions for stability derivatives. However, the evaluation becomes rather unwieldy for bodies with arbitrary meridian profiles.

This report presents a linearized approach which allows the derivation of closed-form expressions for the stability derivatives. By using body-fixed coordinates, a solution to the first-order potential equation is sought. For this purpose the velocity potential, as given by Dorrance [3], is expanded in an elementary fashion for small radial distances from the body. Such an expansion is equivalent to the iterative method of Adams-Sears [20] so that the doublet strength may be obtained in closed form. This procedure provides a consistent generalization over slender-body theory, which is the first term in the expansion and hence prompts the name "quasi-slender body theory." The higher order terms represent the dependence of the solution on Mach number and body geometry.

The present work considers only the next higher order term beyond slender-body theory, i.e., only two terms in the Adams-Sears iteration. One of the chief aims in the derivation given here is to achieve "consistency" in the sense that all so-called second-order terms which arise from the velocity potential and pressure coefficient will be included in the stability derivatives.

To date, for bodies of revolution, the Adams-Sears method has been applied to only one configuration, the slowly oscillating convex parabolic ogive body, in transonic flow by Landahl [6] and supersonic flow by Zartarian-Ashley [7]. In both of these treatments the aerodynamic forces were obtained by "linearized" momentum considerations.

The expressions for stability derivatives which are worked out in this report are applicable to smooth slender pointed-nose bodies of revolution with arbitrary meridian profile. Three numerical examples are given to illustrate the effects of Mach number, differing body geometry and thickness ratio. These examples are a cone, a convex parabolic ogive, and a concave parabolic ogive. Several comparisons of the present results with other theories are presented also.

In the following treatment, dimensionless variables are used with distances referred to body length, ℓ^*, velocities to free stream speed, U^*, velocity potentials to product of body length with free stream speed, and time to body length divided by free stream speed. Starred quantities are dimensional, whereas unstarred quantities are dimensionless.

PROBLEM FORMULATION

Potential Equation

Consider a harmonically pitching pointed body of revolution which is set in a steady uniform supersonic stream. Both the amplitude and frequency of oscillation are assumed to be small. A body-fixed cylindrical coordinate system, as shown in Figure 1, is used to describe the problem. The body is required to be sufficiently slender so that shock wave effects are negligible. Therefore, a velocity potential $\Omega\ (x, r, \theta, t)$ exists. Following Revell [14] a body-fixed perturbation potential $\Phi\ (x, r, \theta, t)$ may be defined by

$$\Omega\ (x, r, \theta, t) = (x-a)\ \cos\ \delta + r\ \sin\ \delta\ \cos\ \theta + \Phi\ (x, r, \theta, t), \tag{1}$$

where

$$\delta = \delta_0\ \cos\ k\,t\ = \left(\delta_0\, e^{ikt} \right)_R$$

The velocity components in the (x, r, θ) directions are then given by

$$\left.\begin{aligned} u &= \Omega_x = \cos\ \delta + \Phi_x \\ v &= \Omega_r = \sin\ \delta \cos\ \theta + \Phi_r \\ w &= \frac{1}{r}\ \Omega_\theta = -\sin\ \delta\ \sin\ \theta + \frac{1}{r}\ \Phi_\theta \end{aligned}\right\} . \tag{2}$$

Nonlinear terms in the potential equation will be neglected in the following treatment. With this restriction Φ is considered to be governed by the first-order unsteady equation.

$$\beta^2\ \Phi_{xx} - \Phi_{rr} - \frac{1}{r}\ \Phi_r - \frac{1}{r^2}\ \Phi_{\theta\theta} + M^2\ (2\ \Phi_{xt} + \Phi_{tt}) = 0. \tag{3}$$

For steady flow the superiority of the first-order equation over the linearized equation has been established by Van Dyke [21]. For unsteady flow, to the authors' knowledge, this point has not been established so that the superiority of equation (3) must be taken as tentative.

In this treatment body-fixed axes have been chosen because the tangency condition and pressure coefficient are less cumbersome to apply than in a wind-fixed coordinate system. The wind-fixed system is complicated by the zero angle-of-attack solution entering into the cross-flow boundary conditions through the

Taylor series transferral of the tangency condition from the pitching body to the mean body [22]. In a body-fixed system this complication is absent.

For small amplitude and low frequencies, following C. Heinz [23], the perturbation potential may be written

$$\Phi(x,r,\theta,t) = \phi(x,r) + [\,\delta \cdot \psi\,(x,r) + \dot{\delta} \cdot \lambda\,(x,r)\,] \cos\theta, \tag{4}$$

where $\dot{\delta} = (ik\delta)_R$, ϕ is the steady-state zero angle-of-attack perturbation potential, and ψ and λ are the in-phase and out-of-phase cross-flow perturbation potentials, respectively.

Boundary Conditions

Upstream of the body all perturbations vanish; hence,

$$\phi = \psi = \lambda = 0 \qquad \text{for } x - \beta r \leq 0 \tag{5}$$

$$\phi_x = \psi_x = \lambda_x = 0 \qquad \text{for } x - \beta r = 0 \tag{6}$$

In addition, the flow must be tangent to the body, which in body-fixed coordinates may be expressed as

$$\left.\begin{aligned} \phi_r &= R'(x) \cdot (1 + \phi_x) \\ \psi_r &= -1 + R'(x) \cdot \psi_x \\ \lambda_r &= -\,[\,(x-a) + R(x)\,R'(x)\,] + R'(x) \cdot \lambda_x \end{aligned}\right\} \text{ at } r = R(x). \tag{7}$$

These are the so-called exact tangency conditions for a non-deforming body.

Normal Force and Pitching Moment

The normal force and pitching moment, referred to the body base area $Q^*(\ell^*) = \pi \epsilon^2 \ell^{*2}$ and body length ℓ^*, are given by the relations

$$C_N = -\frac{2}{Q(1)} \int_0^1 \int_0^\pi R\, C_p(x,R,\theta,t) \cos\theta \, d\theta \, dx \tag{8}$$

and

$$C_M = \frac{2}{Q(1)} \int_0^1 \int_0^\pi (x-a)\, R\, C_p(x,R,\theta,t) \cos\theta \; d\theta\, dx$$

$$+ \frac{2}{Q(1)} \int_0^1 \int_0^\pi R^2 R' C_p(x,R,\theta,t) \cos\theta \; d\theta\, dx, \qquad (9)$$

where the pitching moment is taken about an axis at x = a. The last integral in the moment coefficient is the contribution of forces parallel to the body axis.

Analogous to the expansion of the perturbation potential Φ, the pressure coefficient may be expanded for small frequency and amplitude:

$$C_p(x,R,\theta,t) = C_{p_0}(x,R) + [\delta\, C_{p_1}(x,R) + \dot{\delta}\, C_{p_2}(x,R)] \cos\theta\,. \qquad (10)$$

Then the normal force and pitching moment reduce to

$$C_N = -\delta \cdot \frac{\pi}{Q(1)} \int_0^1 R\, C_{p_1}(x,R)\, dx - \dot{\delta} \cdot \frac{\pi}{Q(1)} \int_0^1 R\, C_{p_2}(x,R)\, dx \qquad (11)$$

$$C_M = \delta \left[\frac{\pi}{Q(1)} \int_0^1 (x-a)\, R\, C_{p_1}(x,R)\, dx + \frac{\pi}{Q(1)} \int_0^1 R^2 R' C_{p_1}(x,R)\, dx \right]$$

$$+ \dot{\delta} \left[\frac{\pi}{Q(1)} \int_0^1 (x-a)\, R\, C_{p_2}(x,R)\, dx + \frac{\pi}{Q(1)} \int_0^1 R^2 R' C_{p_2}(x,R)\, dx \right]. \qquad (12)$$

The flutter derivatives C_{N_δ}, C_{M_δ}, $C_{N_{\dot{\delta}}}$ and $C_{M_{\dot{\delta}}}$ are just the coefficients of δ and $\dot{\delta}$ in equations (11) and (12).

Expansion of the Pressure Coefficient

The exact isentropic pressure coefficient relation is derived from Bernoulli's equation for unsteady flow [14, 24]:

$$C_p = \frac{2}{\gamma M^2} \left(G^{\frac{\gamma}{\gamma-1}} - 1 \right), \qquad (13)$$

where

$$G = 1 + \frac{\gamma - 1}{2} M^2 \left[1 - \left(u^2 + v^2 + w^2 + 2 \Omega_{\tau} \right) \right] \tag{14}$$

and subscript τ denotes partial differentiation with respect to time in a wind-fixed coordinate system. Revell [14] has shown that for small angles of pitch the partial derivative with respect to τ may be expressed in terms of body-fixed variables by

$$\frac{\partial}{\partial \tau} = \frac{\partial}{\partial t} - \dot{\delta}\, r \cos\theta \frac{\partial}{\partial x} + \dot{\delta} \cdot (x-a) \left[\cos\theta \frac{\partial}{\partial r} - \frac{\sin\theta}{r} \frac{\partial}{\partial \theta} \right] . \tag{15}$$

By using equation (15) together with equation (2), which relates the velocity components to the perturbation potential, and equation (4) for the expansion of the perturbation potential for small amplitude and low frequencies, G becomes

$$G = 1 - \frac{\gamma-1}{2} M^2 \left[F_0 + 2 \left(\delta F_1 + \dot{\delta} F_2 \right) \cos\theta \right], \tag{16}$$

where

$$F_0 = 2 \phi_x + \phi_x^2 + \phi_r^2$$

$$F_1 = \psi_x (1 + \phi_x) + \phi_r (1 + \psi_r)$$

$$F_2 = \lambda_x (1 + \phi_x) + \psi + \phi_r (\lambda_r + x-a) - r \phi_x .$$

The pressure coefficient may be expanded using the binomial theorem. To first-order in δ and $\dot{\delta}$, this gives

$$C_p = - F_0 \left(1 - \frac{M^2}{4} F_0 \right) - 2 \left(1 - \frac{M^2}{2} F_0 \right) \left(\delta \cdot F_1 + \dot{\delta} \cdot F_2 \right) \cos\theta . \tag{17}$$

We now put the exact tangency conditions, equation (7), into the definitions of F_1 and F_2, then substitute into equation (17) and retain terms up through second-order in Mach number and body thickness. By comparison of this result with equation (10), we obtain the following expressions for the in-phase and out-of-phase lifting pressure coefficients evaluated at the body surface $r = R(x)$.

$$C_{p_1}(x,R) = -2 \psi_x \left[1 - \beta^2 \phi_x + \left(1 - \frac{M^2}{2} \right) R'^2 \right] \tag{18}$$

$$C_{p_2}(x,R) = -2\left\{\lambda_x\left[1 - \beta^2\phi_x + (1 - \frac{M^2}{2})\,R'^2\right]\right.$$
$$\left. + \psi\,(1 - M^2\,\phi_x - \frac{M^2}{2}\,R'^2) - RR'^2 - R\,\phi_x\right\} \qquad (19)$$

These expressions are consistent with the order to which the potential equation will be solved.

SOLUTION OF THE POTENTIAL EQUATION

Assuming harmonic time dependence,

$$\Phi(x,r,\theta,t) = \phi(x,r) + \hat{\phi}(x,r,\theta)\cdot e^{ikt} \qquad (20)$$

the cross-flow potential $\hat{\phi}(x,r,\theta)$ satisfies

$$\beta^2\,\hat{\phi}_{xx} - \hat{\phi}_{rr} - \frac{1}{r}\,\hat{\phi}_r - \frac{1}{r^2}\,\hat{\phi}_{\theta\theta} + M^2\,(2ik\,\hat{\phi}_x - k^2\,\hat{\phi}) = 0. \qquad (21)$$

The well known dipole solution [25] is

$$\hat{\phi}_{\text{dipole}}(x,r,\theta) = -\frac{\cos\theta}{2\pi}\,\frac{\partial}{\partial r}\left[e^{-i\mu(x-\xi)}\,\frac{\cos\kappa\rho}{\rho}\right] \qquad (22)$$

where

$$\rho = \sqrt{(x-\xi)^2 - \beta^2 r^2}$$

$$\kappa = \frac{k\,M}{\beta^2}$$

$$\mu = \frac{k\,M^2}{\beta^2}$$

By distributing such oscillating dipoles along the x-axis, we obtain the general solution for an oscillating body of revolution,

$$\hat{\phi}(x,r,\theta) = -\frac{\cos\theta}{2\pi}\,\frac{\partial}{\partial r}\int_0^{x-\beta r}\frac{F(\xi)\cos\kappa\rho}{\rho}\,e^{-i\mu(x-\xi)}\,d\xi\,, \qquad (23)$$

where $F(\xi)$ is the dipole distribution which must be determined from the boundary conditions at the body surface.

For a slowly oscillating body of revolution, we may expand this solution with respect to the frequency and retain only terms up through the first power of the frequency; thus,

$$\hat{\phi}(x,r,\theta) = -\frac{\cos\theta}{2\pi} \cdot \frac{\partial}{\partial r} \int_0^{x-\beta r} \frac{F(\xi)\,[1 - i\mu(x-\xi)]}{\sqrt{(x-\xi)^2 - \beta^2 r^2}}\, d\xi \,. \tag{24}$$

Dorrance [3] used this form of the potential together with the slender body doublet strength to obtain stability derivatives for pointed bodies in supersonic flow. However, as pointed out by Miles [26], such a procedure is inconsistent and unnecessarily complicated. Proceeding from equation (24) we will derive a more expedient form for the potential which will show the essential equivalence between Dorrance's method and the Adams-Sears approach [20] and thus provide a consistent means of improving on slender body theory.

For this purpose, we expand equation (24) for small distances from the body axis. Equation (24) can be separated into a steady part,

$$\hat{\phi}_R(x,r,\theta) = -\frac{\cos\theta}{2\pi} \frac{\partial}{\partial r} \int_0^{x-\beta r} \frac{F(\xi)}{\sqrt{(x-\xi)^2 - \beta^2 r^2}}\, d\xi, \tag{25}$$

which represents the potential of a body of revolution at small angle-of-attack, and an unsteady part,

$$\hat{\phi}_I(x,r,\theta) = \frac{\cos\theta}{2\pi} \frac{\partial}{\partial r} \int_0^{x-\beta r} \frac{i\mu \cdot (x-\xi) \cdot F(\xi)}{\sqrt{(x-\xi)^2 - \beta^2 r^2}}\, d\xi \,. \tag{26}$$

The angle-of-attack potential can be expanded by a slight modification of F. Keune's method for the zero angle-of-attack potential [27]. Integrating first the square root expression and taking the partial differentiation outside the integral, we obtain for the zero angle-of-attack potential

$$\phi(x,r) = -\int_0^{x-\beta r} \frac{F(\xi)\, d\xi}{\sqrt{(x-\xi)^2 - \beta^2 r^2}} = -\int_0^{x-\beta r} F(\xi) \cdot \frac{\partial}{\partial x} \ln\left[x - \xi + \sqrt{(x-\xi)^2 - \beta^2 r^2}\right] d\xi$$

$$= -\frac{\partial}{\partial x} \int_0^{x-\beta r} F(\xi) \ln\left[x-\xi + \sqrt{(x-\xi)^2 - \beta^2 r^2}\right] d\xi + F(x-\beta r) \cdot \ln \beta r \,.$$

Expanding this expression for small r gives the familiar slender-body potential:

$$\phi^{(1)}(x,r) = F(x)\ \ln\ \beta r - \frac{\partial}{\partial x}\int_0^x F(\xi)\ \ln\ [2(x-\xi)]\ d\xi\ . \qquad (27)$$

To obtain the next higher approximation, we repeat this process twice for the difference between the exact potential $\phi(x,r)$ and its first approximation $\phi^{(1)}(x,r)$; thus,

$$\phi(x,r) - \phi^{(1)}(x,r) = -\frac{\partial}{\partial x}\int_0^{x-\beta r} F(\xi)\ln\ [x-\xi+\sqrt{(x-\xi)^2-\beta^2 r^2}\ ]\ d\xi$$

$$+\ F(x-\beta r)\cdot\ln\ \beta r - F(x)\ \ln\ \beta r + \frac{\partial}{\partial x}\int_0^x F(\xi)\ \ln\ [2(x-\xi)]\ d\xi$$

$$= -\int_0^{x-\beta r} F'(\xi)\ \frac{\partial}{\partial x}\left\{(x-\xi)\ \ln\ [x-\xi+\sqrt{(x-\xi)^2-\beta^2 r^2}\ ] - \sqrt{(x-\xi)^2-\beta^2 r^2}\right\} d\xi$$

$$+\ F(x-\beta r)\ln\beta r - F(x)\ \ln\ \beta r + \int_0^x F'(\xi)\ \frac{\partial}{\partial x}\ [(x-\xi)\ln\ 2(x-\xi) - (x-\xi)]\ d\xi$$

$$= -\frac{\partial}{\partial x}\int_0^{x-\beta r} F'(\xi)\left\{(x-\xi)\ \ln\ [x-\xi+\sqrt{(x-\xi)^2-\beta^2 r^2}\ ] - \sqrt{(x-\xi)^2-\beta^2 r^2}\right\} d\xi$$

$$+\ F'(x-\beta r)\ \beta r\ \ln\beta r + F(x-\beta r)\ \ln\ \beta r - F(x)\ \ln\ \beta r$$

$$+\ \frac{\partial}{\partial x}\int_0^x F'(\xi)\ [(x-\xi)\ \ln\ 2(x-\xi) - (x-\xi)]\ d\xi$$

$$= -\frac{\partial}{\partial x}\int_0^{x-\beta r} F'(\xi)\ \frac{\partial}{\partial x}\left\{\left(\frac{(x-\xi)^2}{2}+\frac{\beta^2 r^2}{4}\right)\ln\ [x-\xi+\sqrt{(x-\xi)^2-\beta^2 r^2}\ ]\right.$$

$$\left. -\frac{3}{4}\ (x-\xi)\ \sqrt{(x-\xi)^2-\beta^2 r^2}\right\} d\xi + F'(x-\beta r)\cdot\beta r\ \ln\beta r$$

$$+\ F(x-\beta r)\ \ln\beta r - F(x)\ \ln\beta r$$

$$+\ \frac{\partial}{\partial x}\int_0^x F'(\xi)\ \frac{\partial}{\partial x}\left[\frac{(x-\xi)^2}{2}\ \ln\ 2(x-\xi) - \frac{3}{4}\ (x-\xi)^2\right]\ d\xi$$

$$= - \frac{\partial^2}{\partial x^2} \int_0^{x-\beta r} F'(\xi) \left\{ \left(\frac{(x-\xi)^2}{2} + \frac{\beta^2 r^2}{4} \right) \ln \left[x-\xi + \sqrt{(x-\xi)^2 - \beta^2 r^2} \right] \right.$$

$$\left. - \frac{3}{4} (x-\xi) \sqrt{(x-\xi)^2 - \beta^2 r^2} \right\} d\xi + F''(x-\beta r) \cdot \frac{3\beta^2 r^2}{4} \ln \beta r$$

$$+ F'(x-\beta r) \cdot \beta r \ln \beta r + F(x-\beta r) \ln \beta r - F(x) \ln \beta r$$

$$+ \frac{\partial^2}{\partial x^2} \int_0^x F'(\xi) \left[\frac{(x-\xi)^2}{2} \ln 2(x-\xi) - \frac{3}{4} (x-\xi)^2 \right] d\xi . \qquad (28)$$

Using the following expansions,

$$\ln \left[x-\xi + \sqrt{(x-\xi)^2 - \beta^2 r^2} \right] = \ln \left[2(x-\xi) \right] - \frac{1}{4} \frac{\beta^2 r^2}{(x-\xi)^2} + \ldots$$

and

$$\sqrt{(x-\xi)^2 - \beta^2 r^2} = (x-\xi) \left[1 - \frac{1}{2} \frac{\beta^2 r^2}{(x-\xi)^2} + \ldots \right] ,$$

we obtain from equation (28) the following second approximation

$$\phi(x,r) - \phi^{(1)}(x,r) = - \frac{\beta^2 r^2}{4} \frac{\partial^2}{\partial x^2} \int_0^x F'(\xi) \ln \left[2(x-\xi) \right] d\xi$$

$$+ \frac{\beta^2 r^2}{4} F''(x) \left[\ln (\beta r) - 1 \right] . \qquad (29)$$

Inserting this result into equation (25) gives, after differentiation with respect to r, the following near-field approximation for the angle-of-attack potential:

$$\hat{\phi}_R (x,r,\theta) = \frac{\cos\theta}{2\pi r} F(x) + \frac{\cos\theta}{4\pi} r\beta^2 \left[F''(x) \left(\ln \frac{\beta r}{2} - \frac{1}{2} \right) \right.$$

$$\left. - \frac{\partial^3}{\partial x^3} \int_0^x F(\xi) \ln (x-\xi) \, d\xi \right] . \qquad (30)$$

The unsteady part, equation (28), likewise can be approximated by transforming it first into [28]

$$\hat{\phi}_I(x,r,\theta) = \frac{\cos\theta}{2\pi} \frac{\partial}{\partial r} \int_0^{x-\beta r} \frac{i\mu \cdot (x-\xi) \cdot F(\xi)}{\sqrt{(x-\xi)^2 - \beta^2 r^2}} \, d\xi$$

$$= -\frac{\cos\theta}{2\pi} i\mu\beta^2 r \frac{\partial^2}{\partial x^2} \int_0^{x-\beta r} F(\xi) \cosh^{-1}\left(\frac{x-\xi}{\beta r}\right) d\xi \ .$$

This latter expression can be easily approximated for small r in the integrand and in the upper limit

$$\frac{\partial^2}{\partial x^2} \int_0^{x-\beta r} F(\xi) \cosh^{-1}\left(\frac{x-\xi}{\beta r}\right) d\xi = \frac{\partial^2}{\partial x^2} \int_0^{x} F(\xi) \ln\left[\frac{2(x-\xi)}{\beta r}\right] d\xi + \ldots \ .$$

Therefore, the potential of the slowly oscillating body of revolution in supersonic flow, equation (24), may be written in the following form:

$$\hat{\phi}(x,r,\theta) = \left[\frac{F(x)}{2\pi r} + \zeta(x,r;M)\right] \cos\theta, \tag{31}$$

where

$$\zeta(x,r;M) = \frac{r}{4\pi}\beta^2 \left[F''(x)\left(\ln\frac{\beta r}{2} - \frac{1}{2}\right) - F''(0)\ln x - \int_0^x F'''(\xi)\ln(x-\xi)\,d\xi\right] + \frac{ikM^2}{2\pi} r\left[F'(x)\ln\frac{\beta r}{2} - \int_0^x F''(\xi)\ln(x-\xi)\,d\xi\right] .$$

This result also could have been obtained by applying Fourier or Laplace transform techniques to the first-order potential equation and expanding the transformed solution for small distance from the body [7]. The present approach is more elementary and shows at the same time the essential equivalence between Dorrance's approach [3] and the Adams-Sears method [20].

Terms of orders like $\beta^4 \epsilon^5 \ln \beta\epsilon$ have been neglected in equation (31) so that it is consistent with the expressions given earlier for the pressure coefficient.

For convenience we now define a reduced potential $\chi(x,r)$ which follows from equations (4) and (31):

$$\chi(x,r) = \frac{\hat{\phi}(x,r,\theta)}{\cos\theta} = \delta \cdot \psi(x,r) + \dot{\delta} \cdot \lambda(x,r) . \tag{32}$$

The doublet distribution $F(x)$, as mentioned previously, is determined from the tangency condition at the body. Using equation (32) together with equation (7), we may write the exact tangency condition as follows:

$$\frac{\partial \chi}{\partial r} = -W(x) + R'(x) \frac{\partial \chi}{\partial x} \quad \text{at } r = R(x), \tag{33}$$

where for a rigid body

$$W(x) = \delta + \left[x - a + \frac{Q'(x)}{2\pi} \right] \dot{\delta} . \tag{34}$$

The product term in the tangency condition contributes $O(\epsilon^3)$ to the potential function and hence, for consistency, must be retained.

When we apply equation (33), an integral equation for the doublet distributions $F(x)$ is obtained. However, to try to solve this integral equation exactly is inconsistent with the order to which the potential is valid. The correct procedure is to apply the iterative method of Adams-Sears [20]. In keeping with the order to which the potential function, equation (31), is valid, the Adams-Sears iteration consists of two terms only. Therefore, the reduced potential χ may be written

$$\chi = \chi^{(1)} + \chi^{(2)} , \tag{35}$$

and likewise for the doublet distribution,

$$F(x) = F^{(1)}(x) + F^{(2)}(x) . \tag{36}$$

In equations (35) and (36), the first term is the slender-body value, while the second term represents a second-order correction due to Mach number and thickness effects. Substituting equations (35) and (36) into equations (31) and (32) and equating terms of like order gives

$$\left.\begin{aligned} \chi^{(1)}(x,r) &= \frac{F^{(1)}(x)}{2\pi r} \\ \chi^{(2)}(x,r) &= \frac{F^{(2)}(x)}{2\pi r} + \zeta^{(1)}(x,r,M) . \end{aligned}\right\} \tag{37}$$

The body center-line motion function $W(x)$, following the Adams-Sears method, may be written

$$W(x) = W^{(1)}(x) + W^{(2)}(x),$$

where

$$W^{(1)}(x) = \delta + (x-a)\,\dot{\delta}$$

$$W^{(2)}(x) = \frac{Q'(x)}{2\pi}\,\dot{\delta}\ . \qquad (38)$$

Notice that $W^{(1)}(x)$ represents the usual linearized rigid body motion, whereas $W^{(2)}(x)$ represents a higher-order term which enters through oscillation of the body-fixed coordinates and is of the same order as the product term in the tangency condition. Substitution of equations (38) and (35) into equation (33) and equating terms of like order gives the first- and second-order tangency relations:

$$\frac{\partial \chi^{(1)}}{\partial r} = -W^{(1)}(x)$$

$$\frac{\partial \chi^{(2)}}{\partial r} = -W^{(2)}(x) + R'(x)\frac{\partial \chi^{(1)}}{\partial x} \qquad \text{at } r = R(x)\ . \qquad (39)$$

Explicit forms for the first- and second-order doublet distributions follow immediately upon application of the tangency relations, equation (39).

$$F^{(1)}(x) = 2Q(x)\,\delta + 2\,(x-a)\,Q(x)\,\dot{\delta}$$

$$F^{(2)}(x) = \left[2\,Q(x)\,Z_R(x) - \frac{Q'^2(x)}{\pi}\right]\delta + \left[2Q(x)\,Z_I(x) - \frac{1}{\pi}\,(x-a)\,Q'^2(x)\right]\dot{\delta}\ , \qquad (40)$$

where

$$Z_R(x) = \frac{\beta^2}{4\pi}\left[Q''(x)\left(\ln\frac{\beta^2 Q(x)}{4\pi} + 1\right) - 2Q''(0)\ln x - 2\int_0^x Q'''(\xi)\ln(x-\xi)\,d\xi\right]$$

$$Z_I(x) = \frac{\beta^2}{4\pi}\left\{\frac{d^2}{dx^2}\left[(x-a)\,Q(x)\right]\left(\ln\frac{\beta^2 Q(x)}{4\pi} + 1\right) + 2\,a\,Q''(0)\ln x\right.$$

$$- 2 \int_0^x \frac{d^3}{d\xi^3} [(\xi-a)\, Q(\xi)] \ln (x-\xi)\, d\xi \Bigg\}$$

$$+ \frac{M^2}{\pi} \left[Q'(x) \left(\frac{1}{2} \ln \frac{\beta^2 Q(x)}{4\pi} + 1 \right) - \int_0^x Q''(\xi) \ln (x-\xi)\, d\xi \right] .$$

After some straightforward calculation using equations (40) and (37), we arrive at the following expressions for the in-phase and out-of-phase cross flow perturbation potentials, valid to second-order:

$$\psi^{(1)+(2)}(x,r) = \frac{Q(x)}{\pi r} \left[1 + Z_R(x) \right] - \frac{Q'^2(x)}{2\pi^2 r} + r \ln \frac{\beta r}{2} \cdot V_R(x)$$

$$- r\, Y_R(x) \qquad (41)$$

$$\lambda^{(1)+(2)}(x,r) = \frac{Q(x)}{\pi r} [(x-a) + Z_I(x)] - \frac{(x-a)\, Q'^2(x)}{2\pi^2 r} + r \ln \frac{\beta r}{2} \cdot V_I(x)$$

$$- r\, Y_I(x) , \qquad (42)$$

where

$$V_R(x) = \frac{\beta^2}{2\pi} Q''(x)$$

$$V_I(x) = \frac{\beta^2}{2\pi} \frac{d^2}{dx^2} [(x-a)\, Q(x)] + \frac{M^2}{\pi} Q'(x)$$

$$Y_R(x) = \frac{\beta^2}{4\pi} \left[Q''(x) + 2Q''(0) \ln x + 2 \int_0^x Q'''(\xi) \ln (x-\xi)\, d\xi \right]$$

$$Y_I(x) = \frac{\beta^2}{4\pi} \Bigg\{ \frac{d^2}{dx^2} [(x-a)\, Q(x)] - 2a\, Q''(0) \ln x$$

$$+ 2 \int_0^x \frac{d^3}{d\xi^3} [(\xi-a)\, Q(\xi)] \ln (x-\xi)\, d\xi \Bigg\}$$

$$+ \frac{M^2}{\pi} \int_0^x Q''(\xi) \ln (x-\xi)\, d\xi .$$

STABILITY DERIVATIVE CALCULATIONS

With reference to equations (11) and (12), the four flutter derivatives are given by

$$C_{N_\delta} = \left(\frac{\partial C_N}{\partial \delta}\right)_{\delta \to 0} = -\frac{\pi}{Q(1)} \int_0^1 R\, C_{p_1}\, dx \tag{43}$$

$$C_{M_\delta} = \left(\frac{\partial C_M}{\partial \delta}\right)_{\delta \to 0} = \frac{\pi}{Q(1)} \int_0^1 (x-a)\, R\, C_{p_1}\, dx + \frac{\pi}{Q(1)} \int_0^1 R^2\, R'\, C_{p_1}\, dx \tag{44}$$

$$C_{N_{\dot\delta}} = \left(\frac{\partial C_N}{\partial \dot\delta}\right)_{\dot\delta \to 0} = -\frac{\pi}{Q(1)} \int_0^1 R\, C_{p_2}\, dx \tag{45}$$

$$C_{M_{\dot\delta}} = \left(\frac{\partial C_M}{\partial \dot\delta}\right)_{\dot\delta \to 0} = \frac{\pi}{Q(1)} \int_0^1 (x-a)\, R\, C_{p_2}\, dx + \frac{\pi}{Q(1)} \int_0^1 R^2\, R'\, C_{p_2}\, dx \,. \tag{46}$$

The flutter derivatives are related to the stability derivatives by (cf. pp. 16-17 of Reference 24)

$$\left.\begin{aligned} C_{N_\delta} &= C_{N_\alpha} \\ C_{M_\delta} &= C_{M_\alpha} \\ C_{N_{\dot\delta}} &= C_{N_{\dot\alpha}} + C_{N_q} \\ C_{M_{\dot\delta}} &= C_{M_{\dot\alpha}} + C_{M_q} \end{aligned}\right\} \tag{47}$$

Numerous researchers in the past [3, 4, 5] have attempted to compute Mach number and thickness effects on stability derivatives by considering only the linearized form of the pressure coefficient:

$$\left.\begin{aligned} C_{p_1} &= -2\,\psi_x^{(1)+(2)} \\ C_{p_2} &= -2\,(\lambda_x + \psi)^{(1)+(2)} \end{aligned}\right\} \quad \text{at } r = R(x). \tag{48}$$

However, such a procedure is incomplete because the various quadratic terms in equations (18) and (19) together with the terms in the potential arising from the second-order tangency condition are all of comparable order to the thickness and Mach number terms in equation (48).

To obtain all of the second-order terms we evaluate the pressure coefficient derivatives at $r = R(x)$ as follows:

$$\left.\begin{aligned} C_{p_1} &= -2\,\psi_x^{(1)+(2)} + 2\,\beta^2\,\psi_x^{(1)}\,\phi_x^{(1)} - 2\left(1 - \frac{M^2}{2}\right) R'^2(x)\,\psi_x^{(1)} \\ C_{p_2} &= -2\,(\lambda_x + \psi)^{(1)+(2)} + 2\,[\beta^2\,\lambda_x^{(1)} + M^2\,\psi^{(1)} + R(x)]\,\phi_x^{(1)} \\ &\quad - 2\,R'^2(x)\left[\left(1 - \frac{M^2}{2}\right)\lambda_x^{(1)} - \frac{M^2}{2}\,\psi^{(1)} - R(x)\right] \end{aligned}\right\} \tag{49}$$

Needed in the evaluation of C_{p_1} and C_{p_2} are the slender-body potentials $\phi^{(1)}$, $\psi^{(1)}$ and $\lambda^{(1)}$.

$$\phi^{(1)}(x,r) = \frac{Q'(x)}{2\pi} \ln \frac{\beta r}{2} - \frac{1}{2\pi} \frac{\partial}{\partial x} \int_0^x Q'(x) \ln (x-\xi)\, d\xi \tag{50}$$

$$\psi^{(1)}(x,r) = \frac{Q(x)}{\pi r} \tag{51}$$

$$\lambda^{(1)}(x,r) = \frac{(x-a)\,Q(x)}{\pi r}. \tag{52}$$

For conciseness we will evaluate the stability derivatives with the pitch-axis located at the nose of the body, i.e., at a = 0. To compute the stability derivatives for any other pitch-axis location, we simply make use of the following axis transfer relations:

$$\left.\begin{aligned} C_{M_\alpha} &= C_{M_{\alpha_0}} + a\, C_{N_\alpha} \\ C_{N_{\dot\alpha}} + C_{N_q} &= \left(C_{N_{\dot\alpha}} + C_{N_q}\right)_0 - a\, C_{N_\alpha} \\ C_{M_{\dot\alpha}} + C_{M_q} &= \left(C_{M_{\dot\alpha}} + C_{M_q}\right)_0 - a\left[C_{M_\alpha} - \left(C_{N_{\dot\alpha}} + C_{N_q}\right)_0\right] - a^2 C_{N_\alpha} \end{aligned}\right\} \quad (53)$$

where the subscript 0 denotes the derivatives calculated for the pitch-axis at the nose. The above transfer relations follow immediately from the definitions of C_{M_α}, etc., plus the following easily proved relation:

$$C_{p_2}(x,R) = C_{p_{2_0}}(x,R) - a\, C_{p_1}(x,R) . \quad (54)$$

Before giving the stability derivatives, we first derive expressions for the rate of change with x of the in-phase and out-of-phase normal force coefficients. These are given by

$$\frac{d\, C_{N_\alpha}}{d\, x} = -\frac{1}{Q(1)}\, \pi\, R(x)\, C_{p_1}(x,R) \quad (55)$$

$$\frac{d}{d\, x}\left(C_{N_{\dot\alpha}} + C_{N_q}\right)_0 = -\frac{1}{Q(1)}\, \pi\, R(x)\, C_{p_{2_0}}(x,R). \quad (56)$$

Appropriate substitution into equation (49) gives

$$\frac{d\, C_{N_\alpha}}{d\, x} = \frac{1}{Q(1)}\left[\frac{d\, A_R(x)}{d\, x} - 2\, B_R(x) - D_R(x)\right] \quad (57)$$

$$\frac{d}{dx}\left(C_{N_{\dot{\alpha}}} + C_{N_q}\right)_0 = \frac{1}{Q(1)}\left[\frac{dA_I(x)}{dx} + A_R(x) - B_I(x) - C_I(x) - D_I(x)\right]_0 \tag{58}$$

where

$$A_R(x) = Q(x)\left\{2 + \frac{\beta^2}{\pi}\left[Q''(x)\ln\frac{\beta^2 Q(x)}{4\pi} - 2Q''(0)\ln x - 2\int_0^x Q'''(\xi)\ln(x-\xi)\,d\xi\right]\right\}$$

$$B_R(x) = \frac{\beta^2}{\pi}Q'(x)\left[\tfrac{1}{2}Q''(x)\ln\frac{\beta^2 Q(x)}{4\pi} - Q''(0)\ln x - \int_0^x Q'''(\xi)\ln(x-\xi)\,d\xi\right]$$

$$D_R(x) = 2Q'(x)\left[\left(\frac{M^2}{2} - 1\right)R'^2(x) + \frac{1}{\pi}Q''(x)\right]$$

and

$$A_{I_0}(x) = Q(x)\left\langle 2x + \frac{\beta^2}{\pi}\left\{[xQ(x)]''\ln\frac{\beta^2 Q(x)}{4\pi} - 2\int_0^x [\xi Q(\xi)]'''\ln(x-\xi)\,d\xi\right\} + 2\frac{M^2}{\pi}\left[Q'(x)\left(\ln\frac{\beta^2 Q(x)}{4\pi} + 1\right) - 2\int_0^x Q''(\xi)\ln(x-\xi)\,d\xi\right]\right\rangle$$

$$B_{I_0}(x) = \frac{\beta^2}{2\pi}Q'(x)\left\{[xQ(x)]''\ln\frac{\beta^2 Q(x)}{4\pi} - 2\int_0^x [\xi Q(\xi)]'''\ln(x-\xi)\,d\xi\right\} + \frac{M^2}{\pi}Q'(x)\left[Q'(x)\left(\ln\frac{\beta^2 Q(x)}{4\pi} + 1\right) - 2\int_0^x Q''(\xi)\ln(x-\xi)\,d\xi\right]$$

$$C_{I_0}(x) = \frac{1}{\pi}\left[M^2 Q(x) + \frac{\beta^2}{2} x Q'(x)\right]\left[Q''(x) \ln \frac{\beta^2 Q(x)}{4\pi} - 2 Q''(0) \ln x - 2 \int_0^x Q'''(\xi) \ln (x-\xi)\, d\xi\right]$$

$$D_{I_0}(x) = 4\left[\left(1 + \frac{M^2}{2}\right) Q(x) - \frac{1}{2}\left(1 - \frac{M^2}{2}\right) x Q'(x)\right] R'^2(x) + \frac{1}{\pi}\left[x Q'^2(x)\right]'.$$

In the evaluation of the second integral in the moment coefficient, i.e., the moment of forces parallel to the body axis, the slender-body pressure coefficient suffices. Thus,

$$C_{p_1}^{(1)}(x,R) = -4 R'(x) \tag{59}$$

$$C_{p_{2_0}}^{(1)}(x,R) = -4 [x R(x)]'. \tag{60}$$

Performing the required integrations indicated in equations (43) through (46) with a = 0, we arrive at the following expressions for the stability derivatives for pointed-nosed bodies of arbitrary smooth profile:

$$C_{N_\alpha} = 2 + \frac{\beta^2}{\pi}\left[Q''(1) \ln \frac{\beta^2 Q(1)}{4\pi} - 2 \int_0^1 Q'''(x) \ln (1-x)\, dx\right]$$

$$- \frac{\beta^2}{\pi Q(1)}\left[\int_0^1 Q'(x) Q''(x) \ln \frac{\beta^2 Q(x)}{4\pi}\, dx - 2 Q''(0) \int_0^1 Q'(x) \ln x\, dx - 2 \int_0^1 \int_0^x Q'(x) Q'''(\xi) \ln (x-\xi)\, d\xi\, dx\right]$$

$$+ \frac{2}{Q(1)}\left(1 - \frac{M^2}{2}\right) \int_0^1 Q'(x) R'^2(x)\, dx - \frac{Q'^2(1)}{\pi Q(1)}. \tag{61}$$

$$C_{M_{\alpha_0}} = -2 + \frac{2}{Q(1)} \int_0^1 Q(x)\,dx - \frac{\beta^2}{\pi}\left[Q''(1)\,\ln\frac{\beta^2 Q(1)}{4\pi} - 2\int_0^1 Q'''(x)\,\ln(1-x)\,dx\right] + \frac{\beta^2}{\pi Q(1)}\left[\int_0^1 Q(x)\,Q''(x)\ln\frac{\beta^2 Q(x)}{4\pi}\,dx - 2Q''(0)\int_0^1 Q(x)\ln x\,dx - 2\int_0^1\int_0^x Q(x)\,Q'''(\xi)\ln(x-\xi)\,d\xi\,dx\right] + \frac{\beta^2}{\pi Q(1)}\left[\int_0^1 x\,Q'(x)\,Q''(x)\ln\frac{\beta^2 Q(x)}{4\pi}\,dx - 2Q''(0)\int_0^1 x\,Q'(x)\ln x\,dx - 2\int_0^1\int_0^x x\,Q'(x)\,Q'''(\xi)\ln(x-\xi)\,d\xi\,dx\right] - \frac{2}{Q(1)}\left(1-\frac{M^2}{2}\right)\int_0^1 x\,Q'(x)\,R'^2(x)\,dx + \frac{Q'^2(1)}{\pi Q(1)} - \frac{2}{\pi Q(1)}\int_0^1 Q'^2(x)\,dx. \tag{62}$$

$$\left(C_{N_{\dot\alpha}} + C_{N_q}\right)_0 = 2 + \frac{2}{Q(1)}\int_0^1 Q(x)\,dx + \frac{\beta^2}{\pi}\left\{[2Q'(1)+Q''(1)]\ln\frac{\beta^2 Q(1)}{4\pi} - 2\int_0^1 [xQ(x)]'''\ln(1-x)\,dx\right\} + \frac{4M^2}{\pi}\left[\frac{Q'(1)}{2}\left(\ln\frac{\beta^2 Q(1)}{4\pi}+1\right) - \int_0^1 Q''(x)\ln(1-x)\,dx\right] + \frac{\beta^2}{\pi Q(1)}\left[\int_0^1 Q(x)\,Q''(x)\ln\frac{\beta^2 Q(x)}{4\pi}\,dx - 2Q''(0)\int_0^1 Q(x)\ln x\,dx - 2\int_0^1\int_0^x Q(x)\,Q'''(\xi)\ln(x-\xi)\,d\xi\,dx\right]$$

$$
- \frac{\beta^2}{\pi Q(1)} \left[\tfrac{1}{2} \int_0^1 Q'(x) \left[x\, Q(x) \right]'' \ln \frac{\beta^2 Q(x)}{4\pi}\, dx \right.
$$

$$
\left. - \int_0^1 \int_0^x Q'(x) \left[\xi\, Q(\xi) \right]''' \ln (x-\xi)\, d\xi\, dx \right]
$$

$$
- \frac{M^2}{\pi Q(1)} \left[\int_0^1 Q'^2(x) \left(\ln \frac{\beta^2 Q(x)}{4\pi} + 1 \right) dx \right.
$$

$$
\left. - 2 \int_0^1 \int_0^x Q'(x)\, Q''(\xi) \ln (x-\xi)\, d\xi\, dx \right]
$$

$$
- \frac{1}{\pi Q(1)} \left\{ \int_0^1 \left[M^2 Q(x) + \frac{\beta^2}{2} x\, Q'(x) \right] Q''(x) \ln \frac{\beta^2 Q(x)}{4\pi}\, dx \right.
$$

$$
- 2\, Q''(0) \int_0^1 \left[M^2 Q(x) + \frac{\beta^2}{2} x\, Q'(x) \right] \ln x\, dx
$$

$$
\left. - 2 \int_0^1 \int_0^x \left[M^2 Q(x) + \frac{\beta^2}{2} x\, Q'(x) \right] Q'''(\xi) \ln (x-\xi)\, d\xi\, dx \right\}
$$

$$
- \frac{4}{Q(1)} \int_0^1 \left[\left(1 + \frac{M^2}{2} \right) Q(x) - \frac{1}{2} \left(1 - \frac{M^2}{2} \right) x\, Q'(x) \right] R'^2(x)\, dx
$$

$$
- \frac{Q'^2(1)}{\pi Q(1)} \,. \qquad (63)
$$

$$
\left(C_{M_{\dot{\alpha}}} + C_{M_q} \right)_0 = - 2 - \frac{\beta^2}{\pi} \left\{ \left[2\, Q'(1) + Q''(1) \right] \ln \frac{\beta^2 Q(1)}{4\pi} \right.
$$

$$
\left. - 2 \int_0^1 \left[x\, Q(x) \right]''' \ln (1-x)\, dx \right\}
$$

$$
- \frac{4 M^2}{\pi} \left[\frac{Q'(1)}{2} \left(\ln \frac{\beta^2 Q(1)}{4\pi} + 1 \right) - \int_0^1 Q''(x) \ln (1-x)\, dx \right]
$$

$$+\frac{\beta^2}{\pi Q(1)}\left\{\int_0^1 Q(x)\,[x\,Q\,x\,]''\ln\frac{\beta^2 Q(x)}{4\pi}\,dx\right.$$

$$\left.-2\int_0^1\int_0^x Q(x)\,[\xi Q(\xi)]'''\ln(x-\xi)\,d\xi\,dx\right\}$$

$$+\frac{M^2}{\pi}\left[Q(1)\left(\ln\frac{\beta^2 Q(1)}{4\pi}+\frac{1}{2}\right)-\frac{4}{Q(1)}\int_0^1\int_0^x Q(x)\,Q''(\xi)\ln(x-\xi)\,d\xi\,dx\right]$$

$$-\frac{\beta^2}{\pi Q(1)}\left[\int_0^1 x\,Q(x)\,Q''(x)\ln\frac{\beta^2 Q(x)}{4\pi}\,dx\right.$$

$$-2\,Q''(0)\int_0^1 x\,Q(x)\ln x\,dx$$

$$\left.-2\int_0^1\int_0^x x\,Q(x)\,Q'''(\xi)\ln(x-\xi)\,d\xi\,dx\right]$$

$$+\frac{\beta^2}{\pi Q(1)}\left[\frac{1}{2}\int_0^1 x\,Q'(x)\,[x\,Q(x)]''\ln\frac{\beta^2 Q(x)}{4\pi}\,dx\right.$$

$$\left.-\int_0^1\int_0^x x\,Q'(x)\,[\xi\,Q(\xi)]'''\ln(x-\xi)\,d\xi\,dx\right]$$

$$+\frac{M^2}{\pi Q(1)}\left[\int_0^1 x\,Q'^2(x)\left(\ln\frac{\beta^2 Q(x)}{4\pi}+1\right)dx\right.$$

$$\left.-2\int_0^1\int_0^x x\,Q'(x)\,Q''(\xi)\ln(x-\xi)\,d\xi\,dx\right]$$

$$+\frac{1}{\pi Q(1)}\left\{\int_0^1\left[M^2 Q(x)+\frac{\beta^2}{2}\,x\,Q'(x)\right]x\,Q''(x)\ln\frac{\beta^2 Q(x)}{4\pi}\,dx\right.$$

$$\left.-2\,Q''(0)\int_0^1\left[M^2 Q(x)+\frac{\beta^2}{2}\,x\,Q'(x)\right]x\ln x\,dx\right.$$

$$- 2\int_0^1 \int_0^x \left[M^2 Q(x) + \frac{\beta^2}{2} x Q'(x) \right] x Q'''(\xi) \ln (x-\xi)\, d\xi\, dx \Bigg\}$$

$$+ \frac{1}{\pi Q(1)} \left(\frac{M^2}{2} - 1 \right) \int_0^1 x Q'(x) \left[Q'(x) + 2\pi x R'^2(x) \right] dx$$

$$+ \frac{Q'^2(1)}{\pi Q(1)} - \frac{Q(1)}{\pi} . \qquad (64)$$

NUMERICAL RESULTS AND DISCUSSION

Application to Specific Body Shapes

To illustrate the effect of differing body geometry on the stability derivatives, numerical examples were worked out for three typical pointed bodies of revolution. These are as follows:

1. Right-circular cone, $R(x) = \epsilon x$

2. Convex parabolic ogive, $R(x) = \epsilon x(2-x)$

3. Concave parabolic ogive, $R(x) = \frac{\epsilon x}{2}(1+x)$.

These bodies were chosen, first, because they possess the three basic types of curvature, and second, to determine whether a similarity exists between the geometric effects for bodies of revolution and low aspect ratio wings. In addition, other theoretical results are available for the cone [29] and convex ogive [7] with which to make comparisons.

The actual evaluation of the expressions for stability derivatives given in the previous section is straightforward, although tedious because of the many integrals which occur. Even for the simple body profiles considered here the number of such integrals is very large, so that the main problem is one of bookkeeping. Some simplification is to be had in the present case because all of the integrals reduce to four basic types, which are listed, together with their integration formulas, in Table I. All required numerical values of the generalized formulas of Table I are listed in Table II.

The final numerical formulas as functions of Mach number and body fineness ratio for the three bodies are given in the Appendix. The present theory can be applied to other smooth bodies, and analytical integration is possible, provided the body area distribution $Q(x)$ is a factorable polynomial. This

restriction arises in the treatment of integrals containing $\ln Q(x)$. From a practical standpoint, the labor involved would be considerable in treating any profile whose radius distribution $R(x)$ is of higher degree than a quadratic.

Discussion of Results

Numerical results for the various stability derivatives according to the present theory were computed for the body shapes described above for three values of body fineness ratio, $\epsilon = 0$, 0.05 and 0.10. The case $\epsilon = 0$ corresponds to pure slender-body theory. A Mach number range from 1.2 to 3.0 was investigated, and a pitch axis location of $a = 0.4$ was chosen.

Plots of C_{N_α} are presented in Figures 2 through 4, C_{M_α} in Figures 5 and 6, $C_{N_{\dot{\alpha}}} + C_{N_q}$ in Figures 7 through 9, and $C_{M_{\dot{\alpha}}} + C_{M_q}$ in Figures 10 and 11. These plots show a significant influence of Mach number and body thickness on the four stability derivatives. For the cone, excellent agreement with the "exact" first-order theory of Tobak-Wehrend [29] is obtained as shown in Figures 2 and 7. In fact, it can be demonstrated by series expansion of equations (40), (45) and (50) of Reference 29 that the present theory, equations (A1) - (A2) of the Appendix, results by retaining second-order terms only. No plots of C_{M_α} or $C_{M_{\dot{\alpha}}} + C_{M_q}$ are given for the cone because the forces and moments are related to each other by the simple exact relations [29] for $a = 0$

$$C_{M_\alpha}{}_0 = -\frac{2}{3}(1+\epsilon^2)\, C_{N_\alpha} \tag{65}$$

$$\left(C_{M_{\dot{\alpha}}} + C_{M_q}\right)_0 = -\frac{3}{4}(1+\epsilon^2)\left(C_{N_{\dot{\alpha}}} + C_{N_q}\right)_0 . \tag{66}$$

In Figures 3 through 6 the in-phase derivatives C_{N_α} and C_{M_α} for the two ogives as given by quasi-slender body theory are compared with an exact method of characteristics solution [30] which superposes a small angle-of-attack perturbation on the nonlinear axisymmetric flow. The agreement for C_{N_α} is good up to a value of the hypersonic similarity parameter $2M\epsilon$ of 0.3. Fair agreement is obtained for the pitching moment coefficient slope C_{M_α}. Better insight

into the behavior of these derivatives is gained by comparing the local normal force distribution $d C_{N_\alpha}/dx$ of the two theories. These comparisons are given for various Mach numbers and fineness ratios in Figures 12 through 19.

Referring to Figures 10 and 11 for pitch damping, we observe the following behavior. For a given set of governing parameters, the concave body, the cone and the convex body (in that order) are progressively more stable. Thus, in general, decreasing the body curvature increases the pitch damping, i.e., $C_{M_{\dot{\alpha}}} + C_{M_q}$ becomes more negative. This behavior is similar to the pitch damping characteristics as a function of leading edge curvature of a thin low aspect ratio wing in transonic flow as shown by Landahl [31].

Three nonlinear studies for the oscillating cone are given in References 14, 15 and 32. Revell's analysis [14] is an extension to unsteady flow of the second-order slender-body theory of Lighthill. The analyses of Brong [15] and Hsu [32], which are somewhat similar to one another, are based on a time-dependent perturbation about the nonlinear Taylor-Maccoll solution [33]. The results of References 14, 15 and 32 for $\left(C_{N_{\dot{\alpha}}} + C_{N_q}\right)_0$ for a cone of 10-degree semi-apex angle are compared in Figure 20 with those of quasi-slender body theory and the first-order "exact" results of Tobak-Wehrend [29]. The agreement between the present results and those of References 29, 15 and 32 is remarkably good up to $2M\epsilon$ of about 0.75, whereupon quasi-slender body theory begins to diverge sharply. The reversal of trends in quasi-slender body theory is similar to the behavior of Revell's second-order theory. By comparison of the two with the "exact" first-order theory of Tobak-Wehrend, further support is given to Revell's conjecture that such trend reversals indicate the breakdown of second-order theory, and by inference, the breakdown of quasi-slender body theory also.

The theory of Zartarian-Ashley for slowly oscillating bodies of revolution in supersonic flow [7], as mentioned earlier, also uses the Adams-Sears procedure to solve for the doublet potential. Their aerodynamic forces are obtained by applying "linearized" momentum considerations, whereas in the present analysis these forces are obtained by integration of the pressures over the body surface. We observe that the present stability derivative results contain those of Reference 7 plus additional Mach number and body thickness terms. This disagreement, at least in part, is attributable to the use in

Reference 7 of the "linearized" momentum relation which, analogous to the use of the "linearized" pressure coefficient, does not give all of the Mach number and body thickness terms.

Finally, it should be noted that the present work is based upon an expansion of the cross-flow potential, equation (23), with respect to frequency. Therefore, the results imply, in addition to the limitations already imposed by linearized theory, that

$$k M << (M - 1)$$

which sets an upper limit to the frequency range and a lower limit to the Mach number range over which the results may be used.

George C. Marshall Space Flight Center,
National Aeronautics and Space Administration
Huntsville, Alabama, November 24, 1965

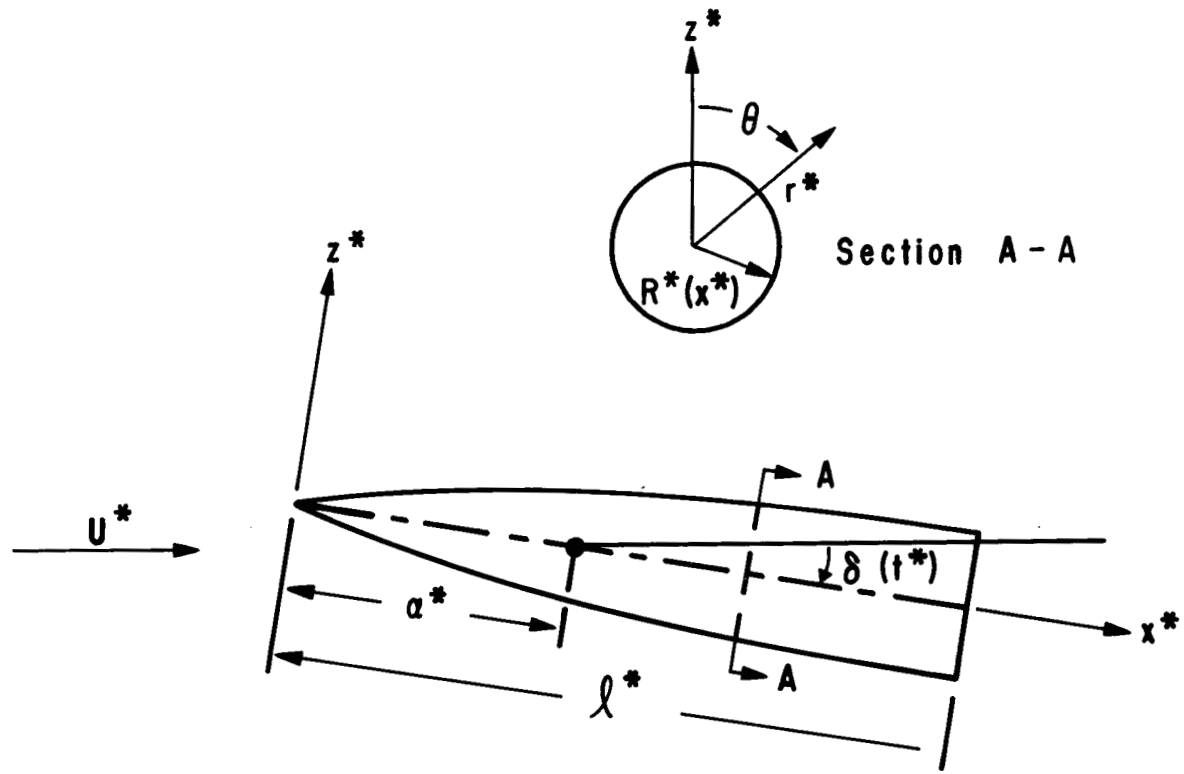

FIGURE 1. BODY FIXED COORDINATE SYSTEM

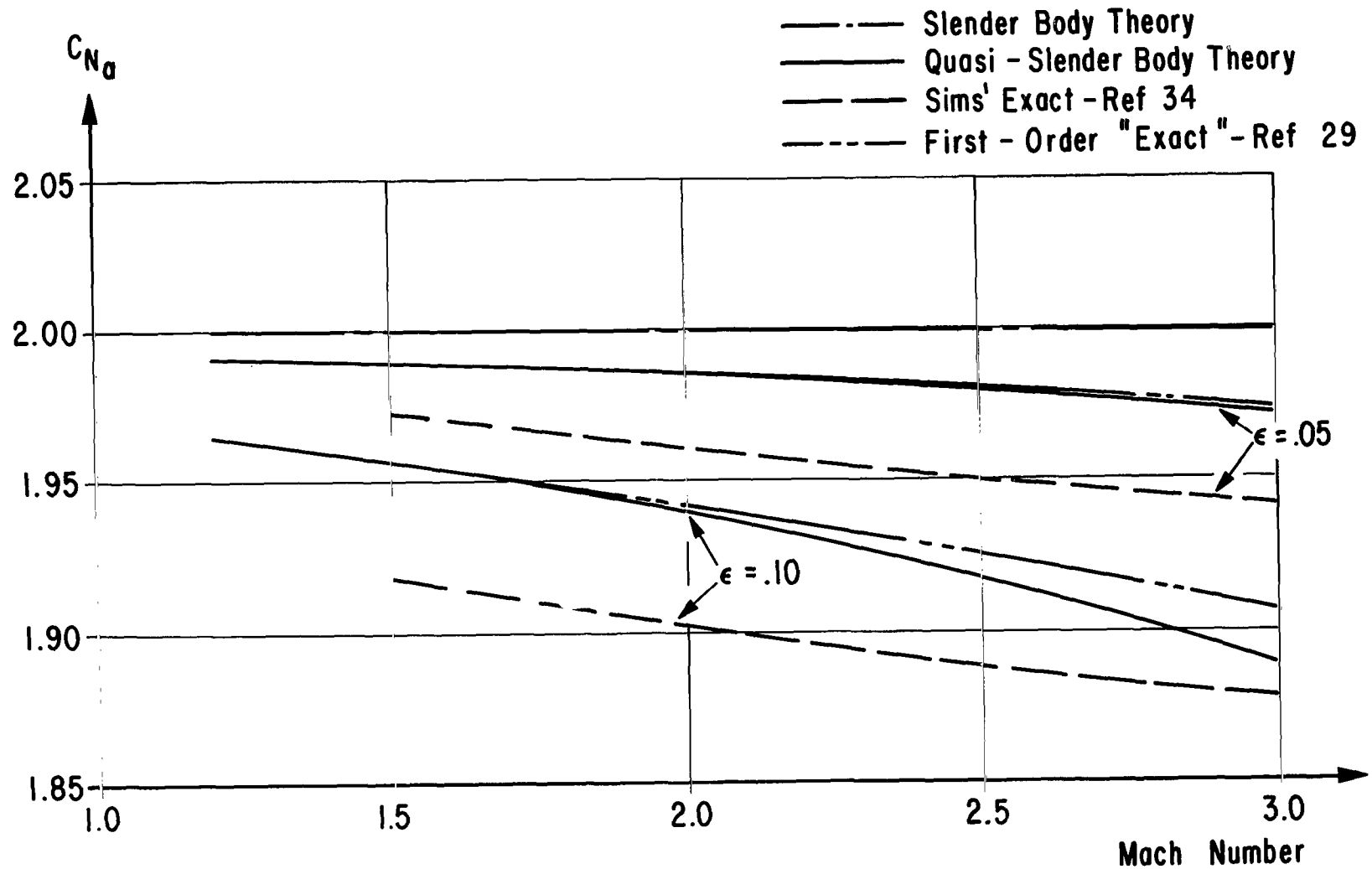

FIGURE 2. EFFECT OF MACH NUMBER AND THICKNESS RATIO ON NORMAL FORCE COEFFICIENT SLOPE FOR A CONE

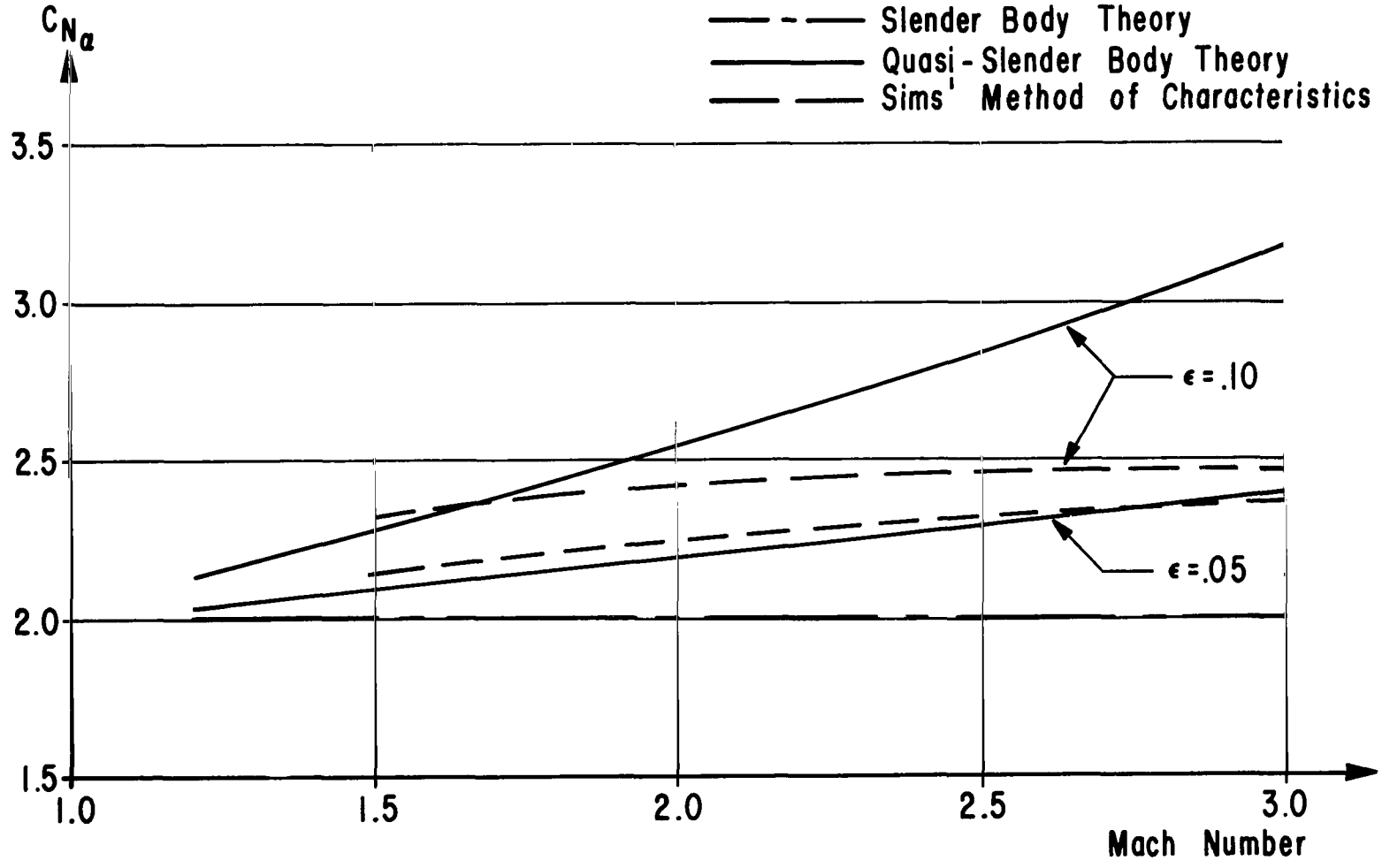

FIGURE 3. EFFECT OF MACH NUMBER AND THICKNESS RATIO ON NORMAL FORCE COEFFICIENT SLOPE FOR A CONVEX PARABOLIC OGIVE

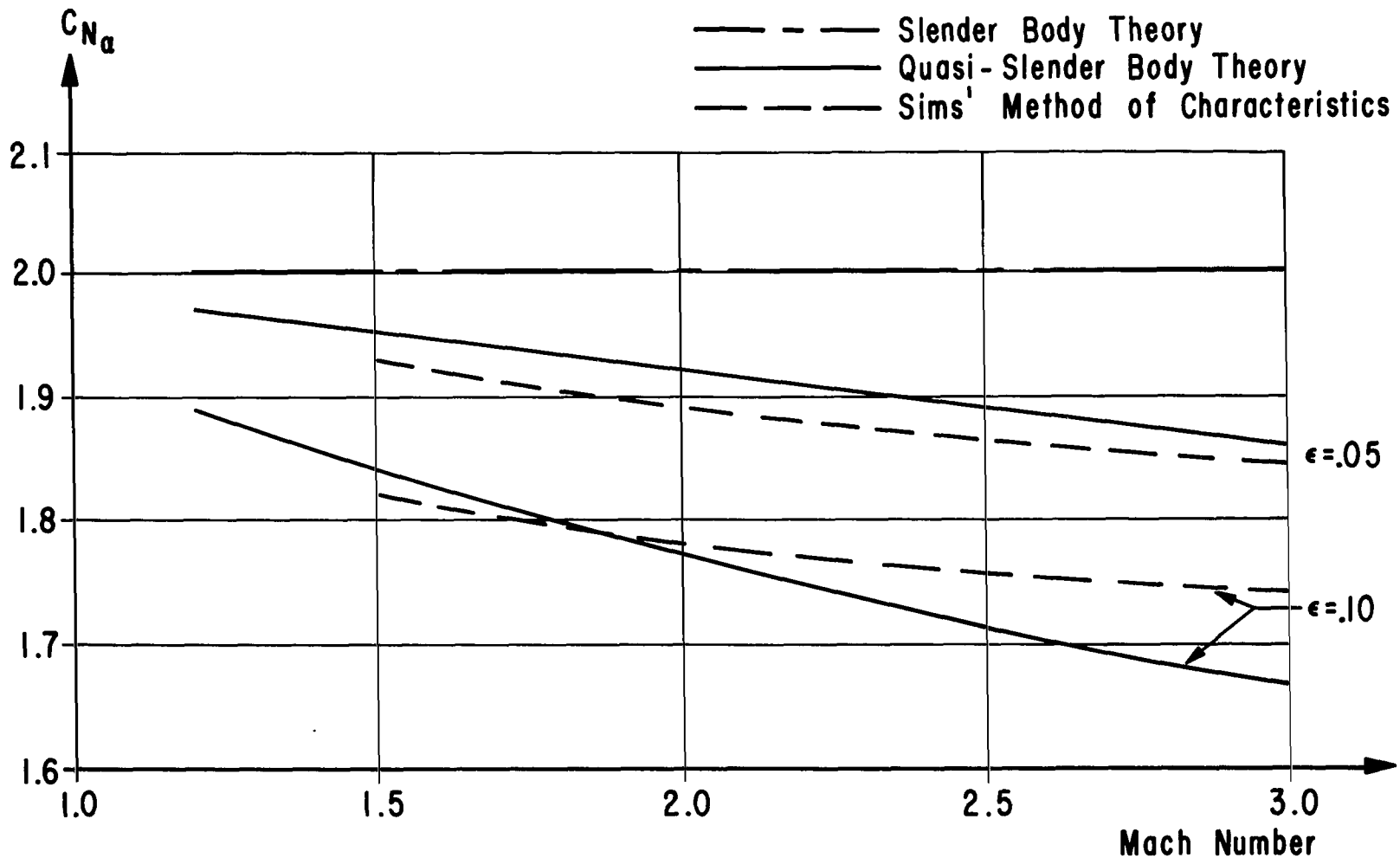

FIGURE 4. EFFECT OF MACH NUMBER AND THICKNESS RATIO ON NORMAL FORCE COEFFICIENT SLOPE FOR A CONCAVE PARABOLIC OGIVE

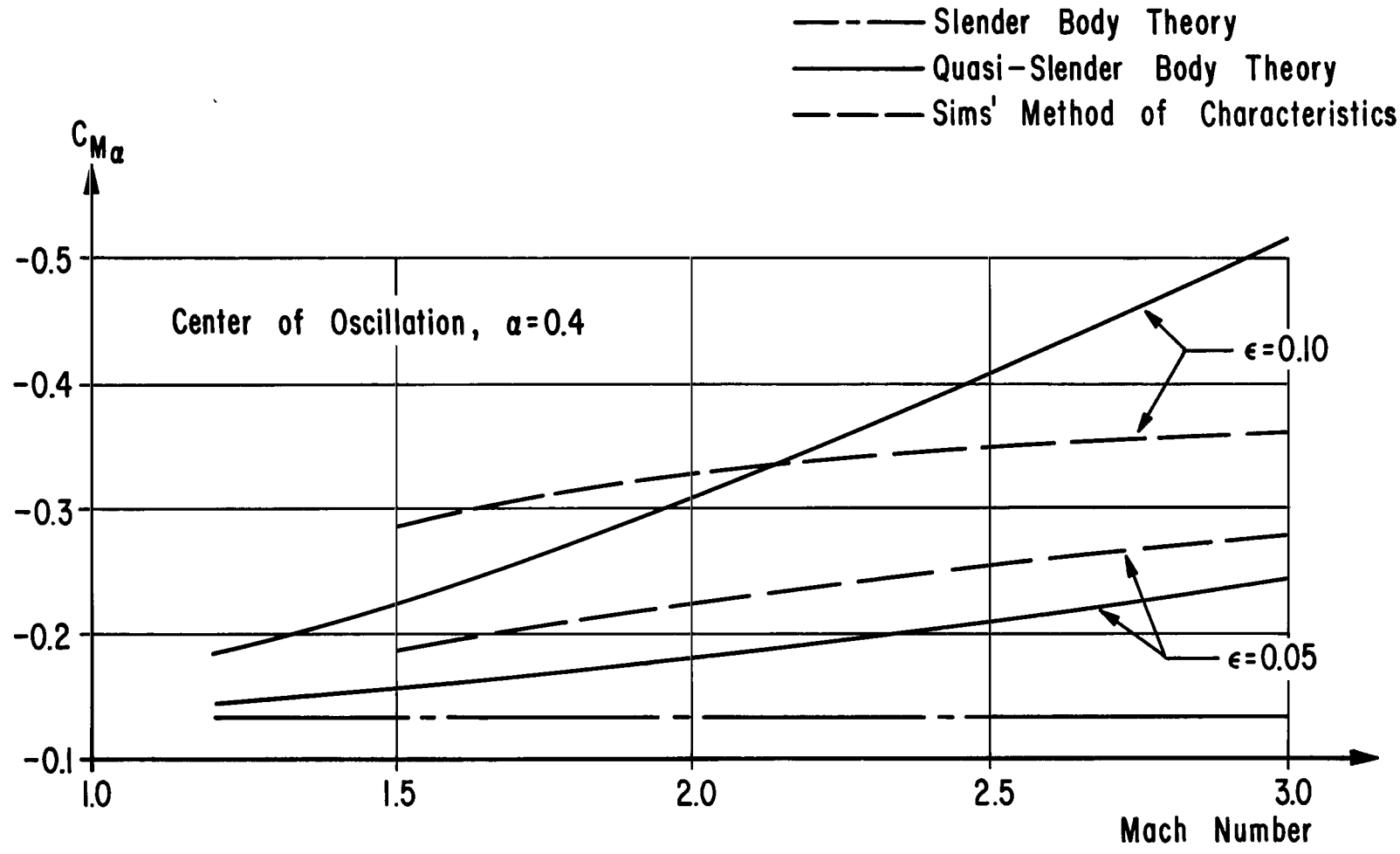

FIGURE 5. EFFECT OF MACH NUMBER AND THICKNESS RATIO ON PITCHING MOMENT COEFFICIENT SLOPE FOR A CONVEX PARABOLIC OGIVE

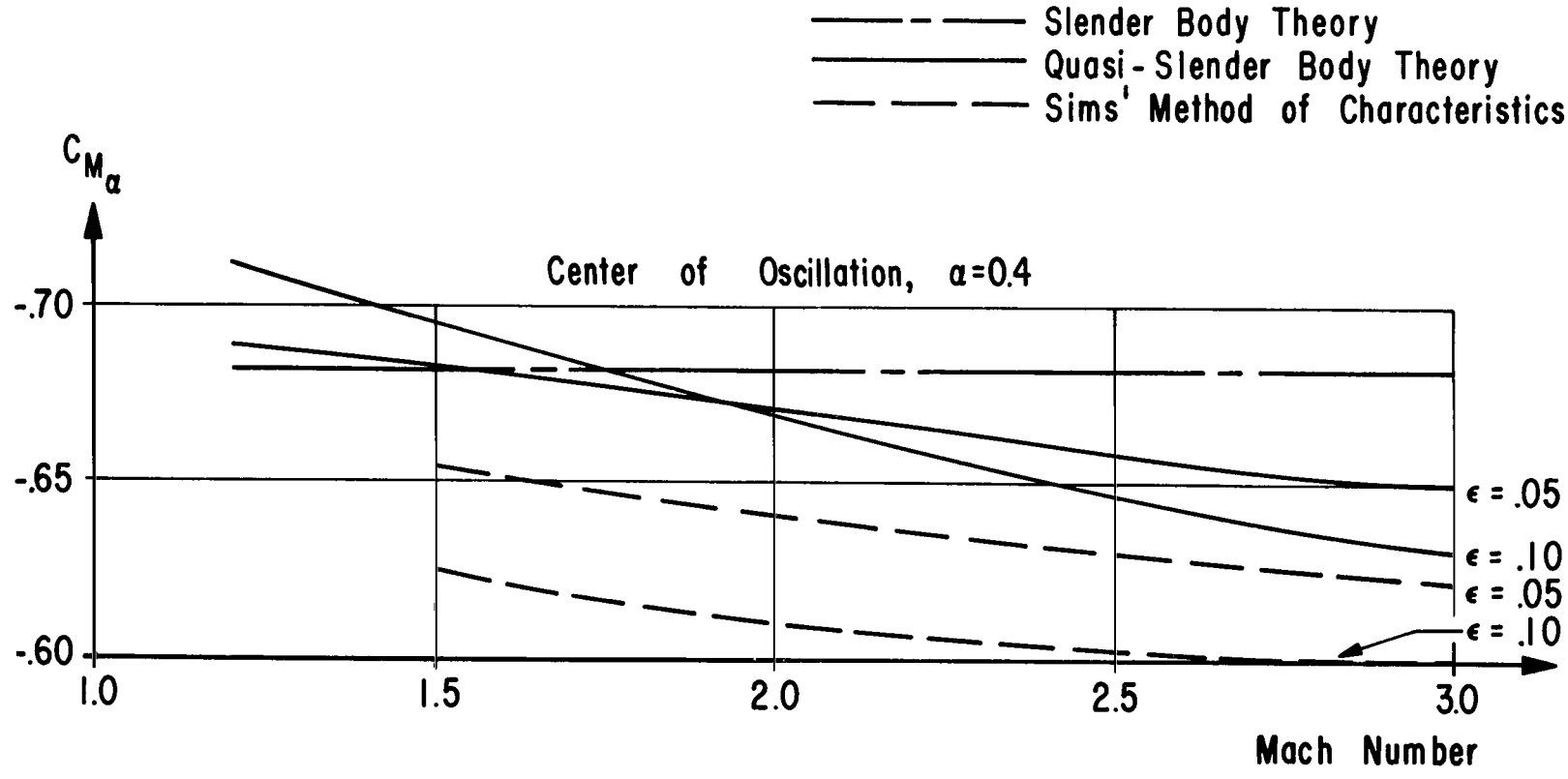

FIGURE 6. EFFECT OF MACH NUMBER AND THICKNESS RATIO ON PITCHING MOMENT COEFFICIENT SLOPE FOR A CONCAVE PARABOLIC OGIVE

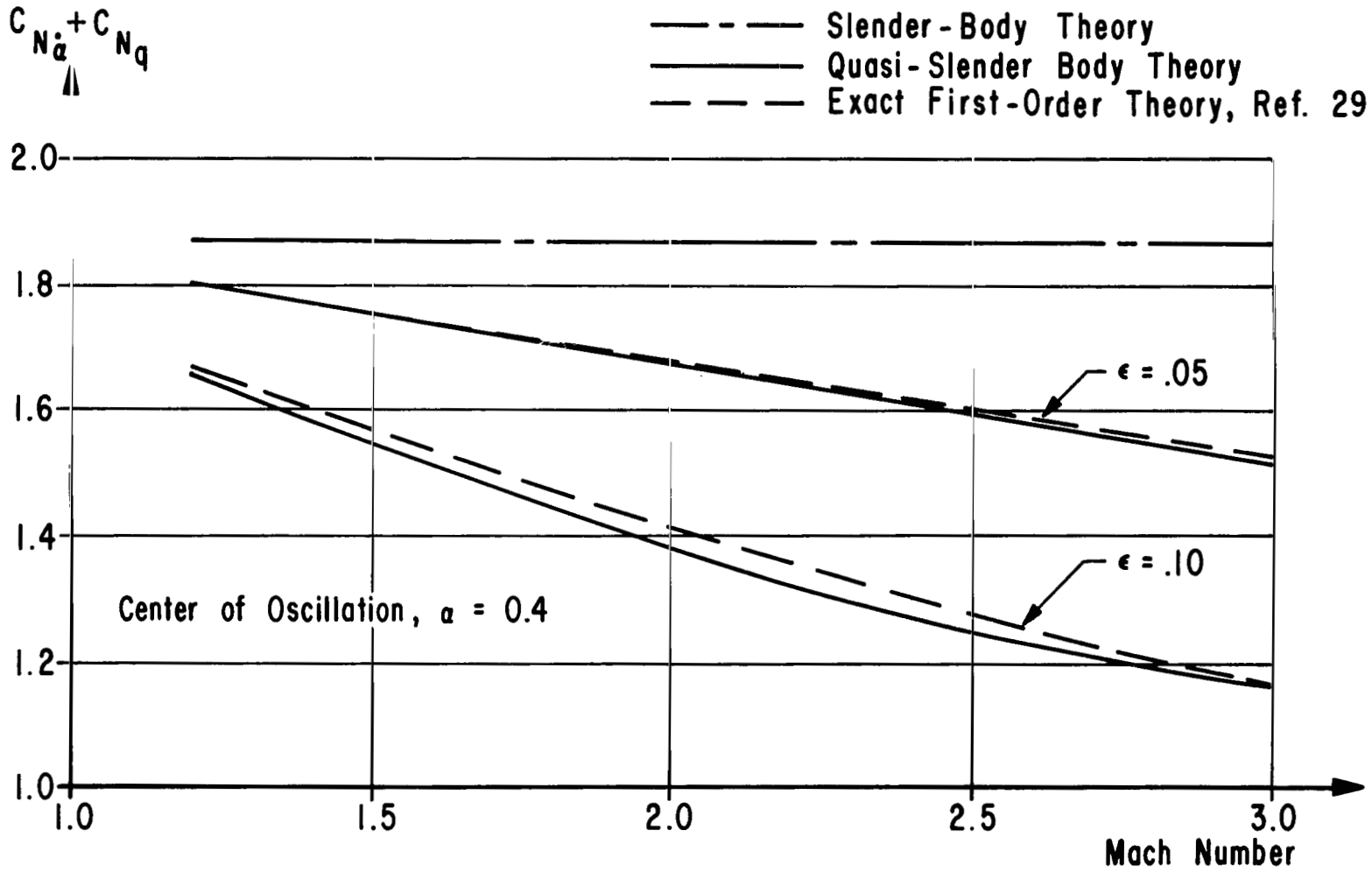

FIGURE 7. EFFECT OF MACH NUMBER AND THICKNESS RATIO ON FIXED AXIS DAMPING IN PITCH NORMAL FORCE COEFFICIENT FOR A CONE

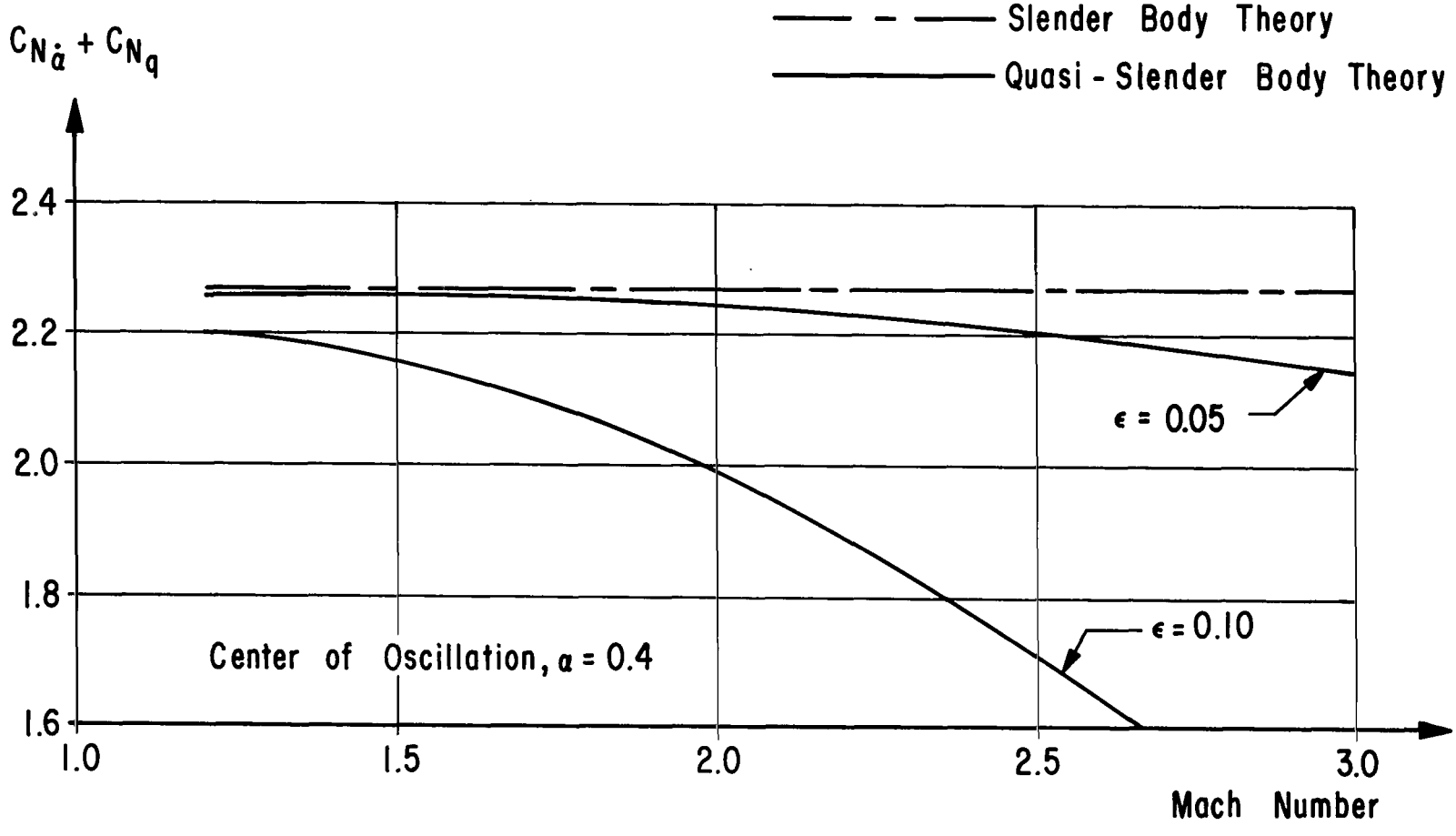

FIGURE 8. EFFECT OF MACH NUMBER AND THICKNESS RATIO ON FIXED AXIS DAMPING IN PITCH NORMAL FORCE COEFFICIENT FOR A CONVEX PARABOLIC OGIVE

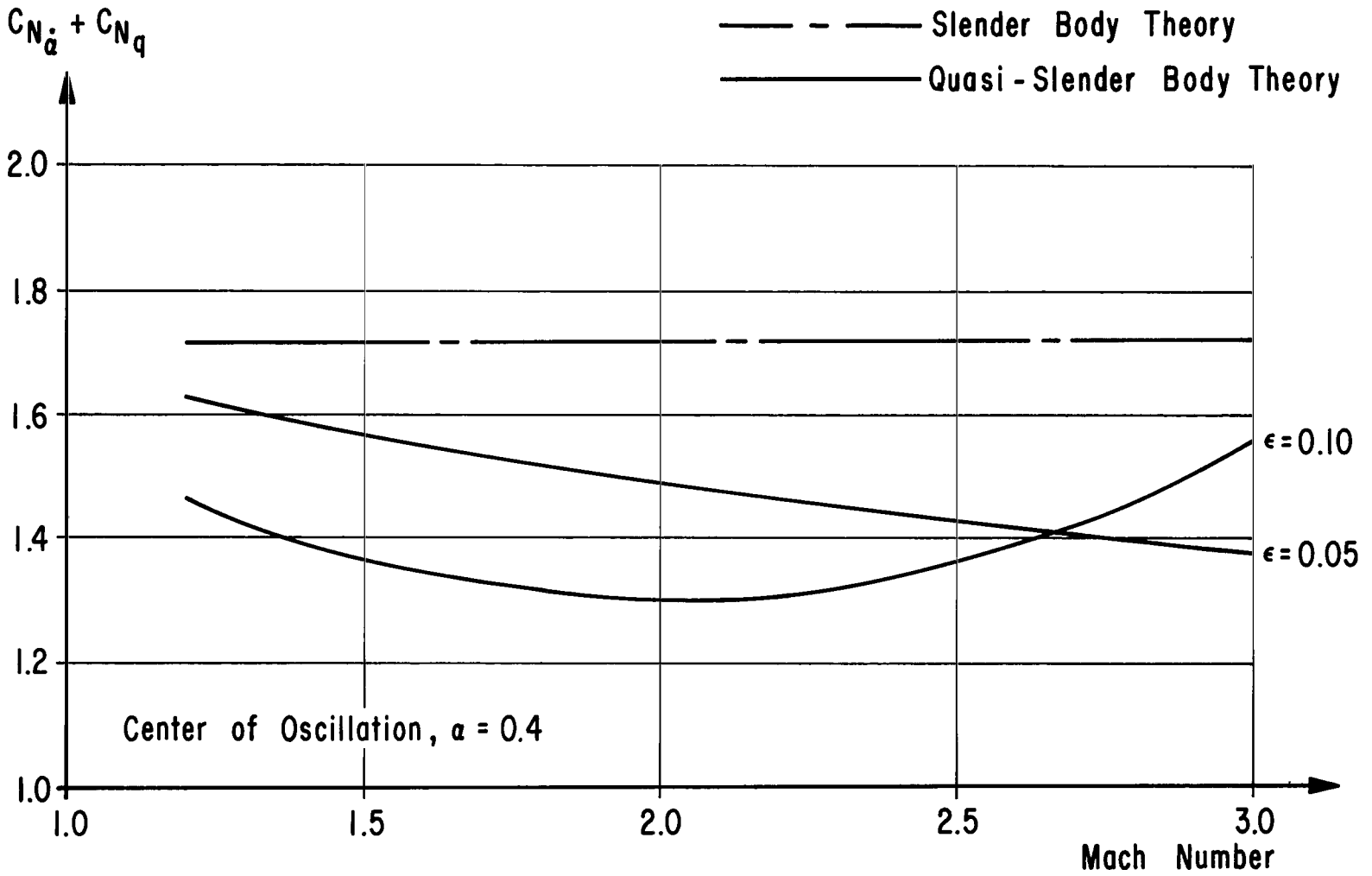

FIGURE 9. EFFECT OF MACH NUMBER AND THICKNESS RATIO ON FIXED AXIS DAMPING IN PITCH NORMAL FORCE COEFFICIENT FOR A CONCAVE PARABOLIC OGIVE

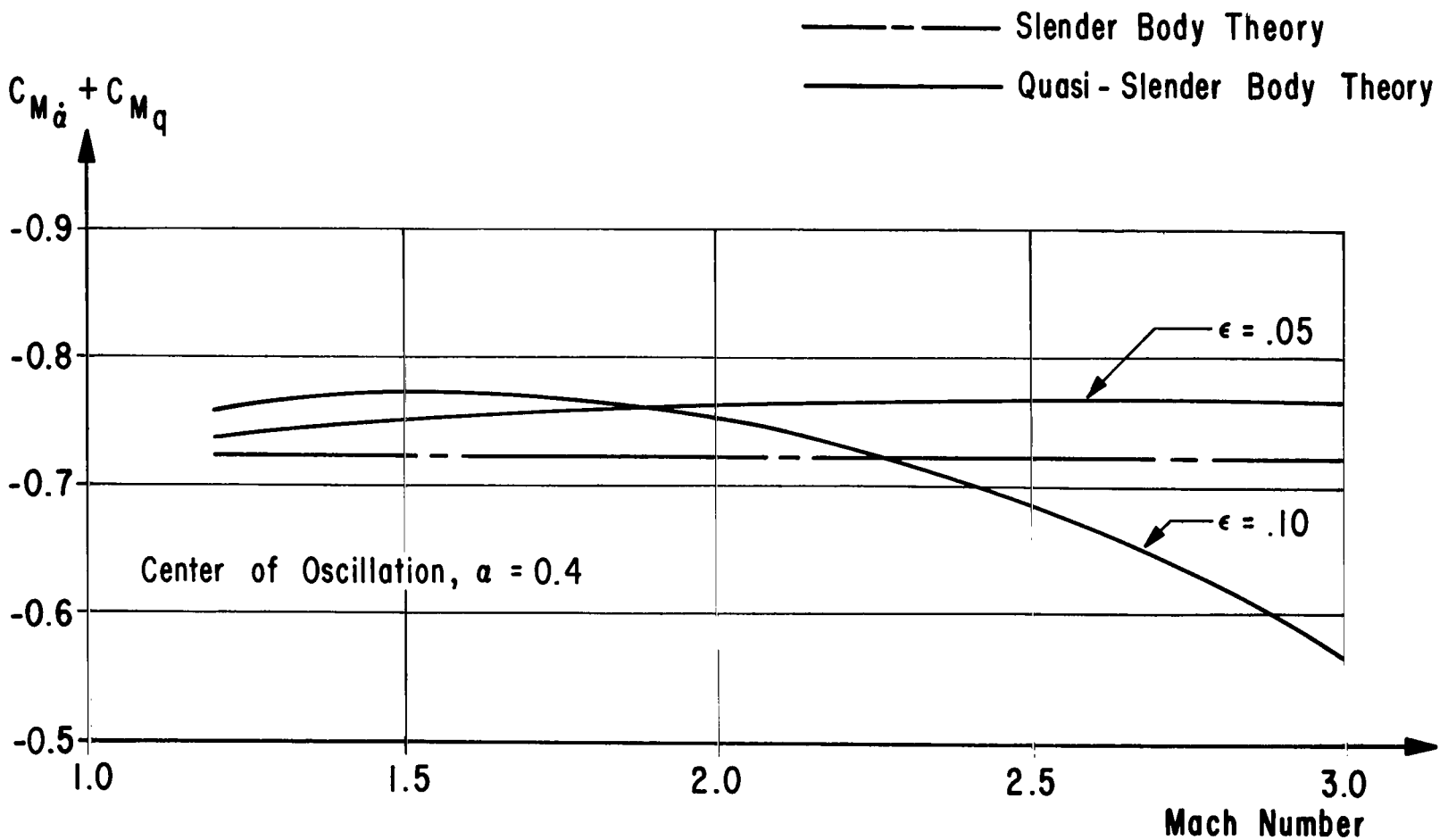

FIGURE 10. EFFECT OF MACH NUMBER AND THICKNESS RATIO ON FIXED AXIS DAMPING IN PITCH MOMENT COEFFICIENT FOR A CONVEX PARABOLIC OGIVE

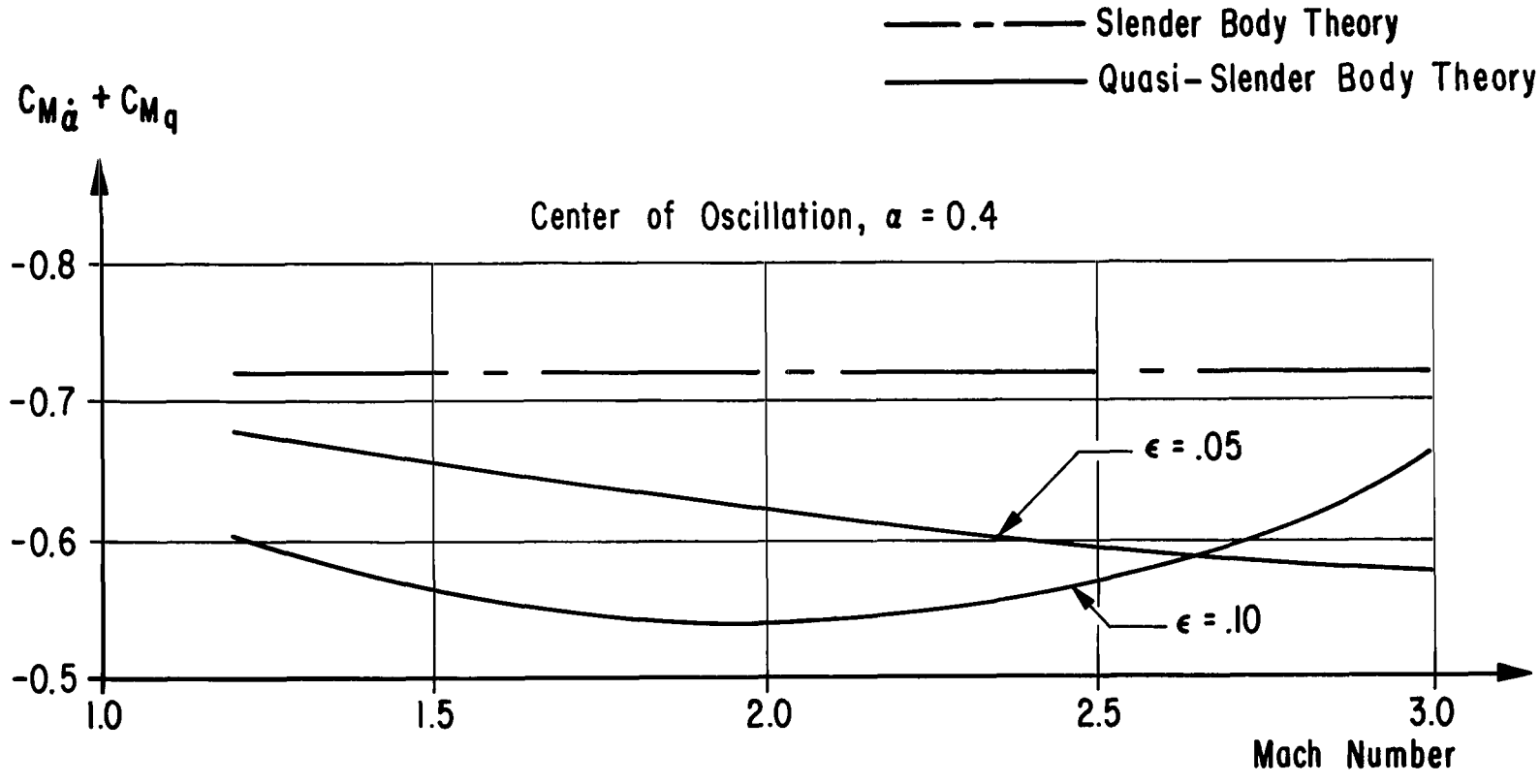

FIGURE 11. EFFECT OF MACH NUMBER AND THICKNESS RATIO ON FIXED AXIS DAMPING IN PITCH MOMENT COEFFICIENT FOR A CONCAVE PARABOLIC OGIVE

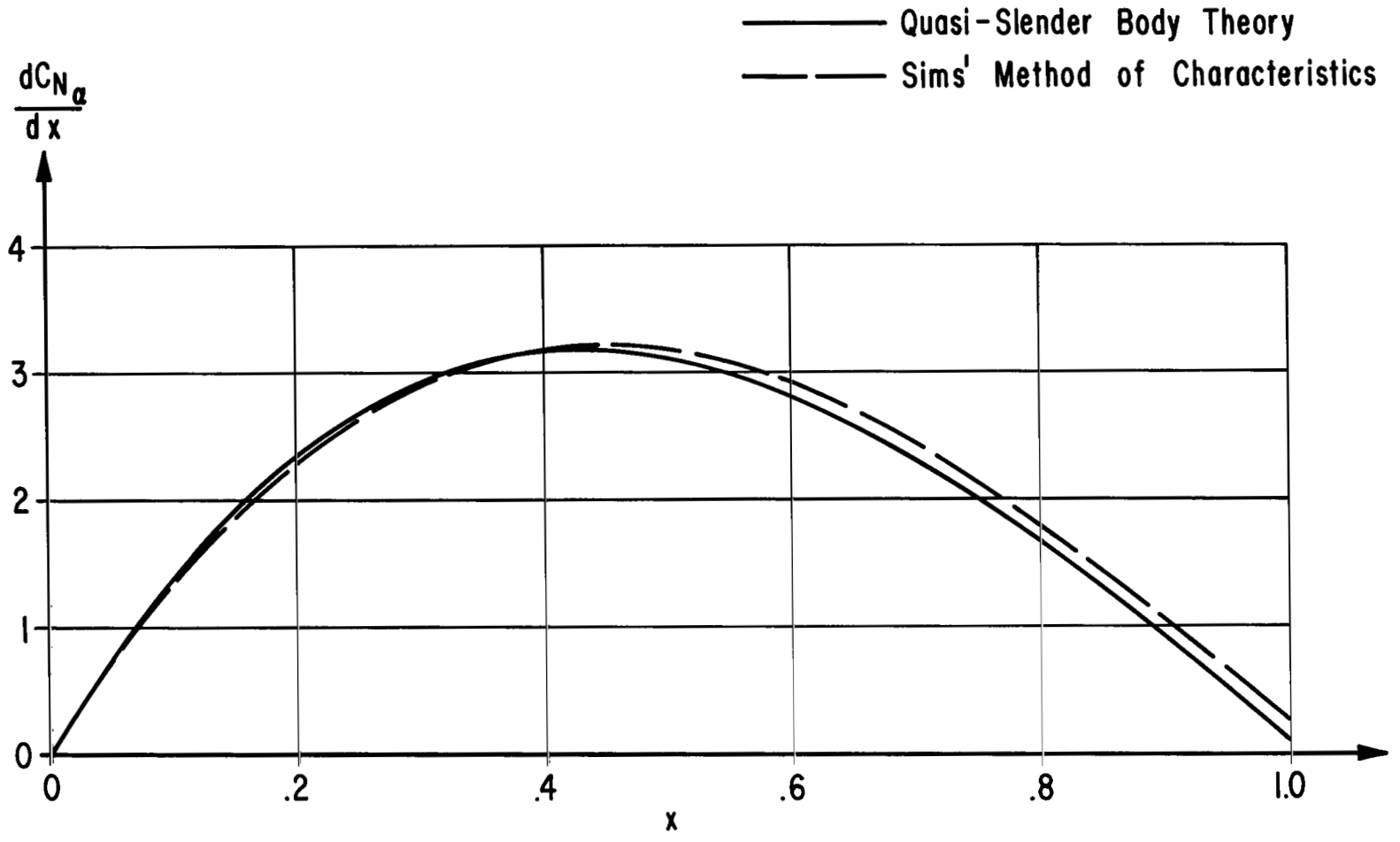

FIGURE 12. LOCAL NORMAL FORCE VARIATION FOR A CONVEX PARABOLIC OGIVE OF FINENESS RATIO 0.05 AT A MACH NUMBER OF 1.5

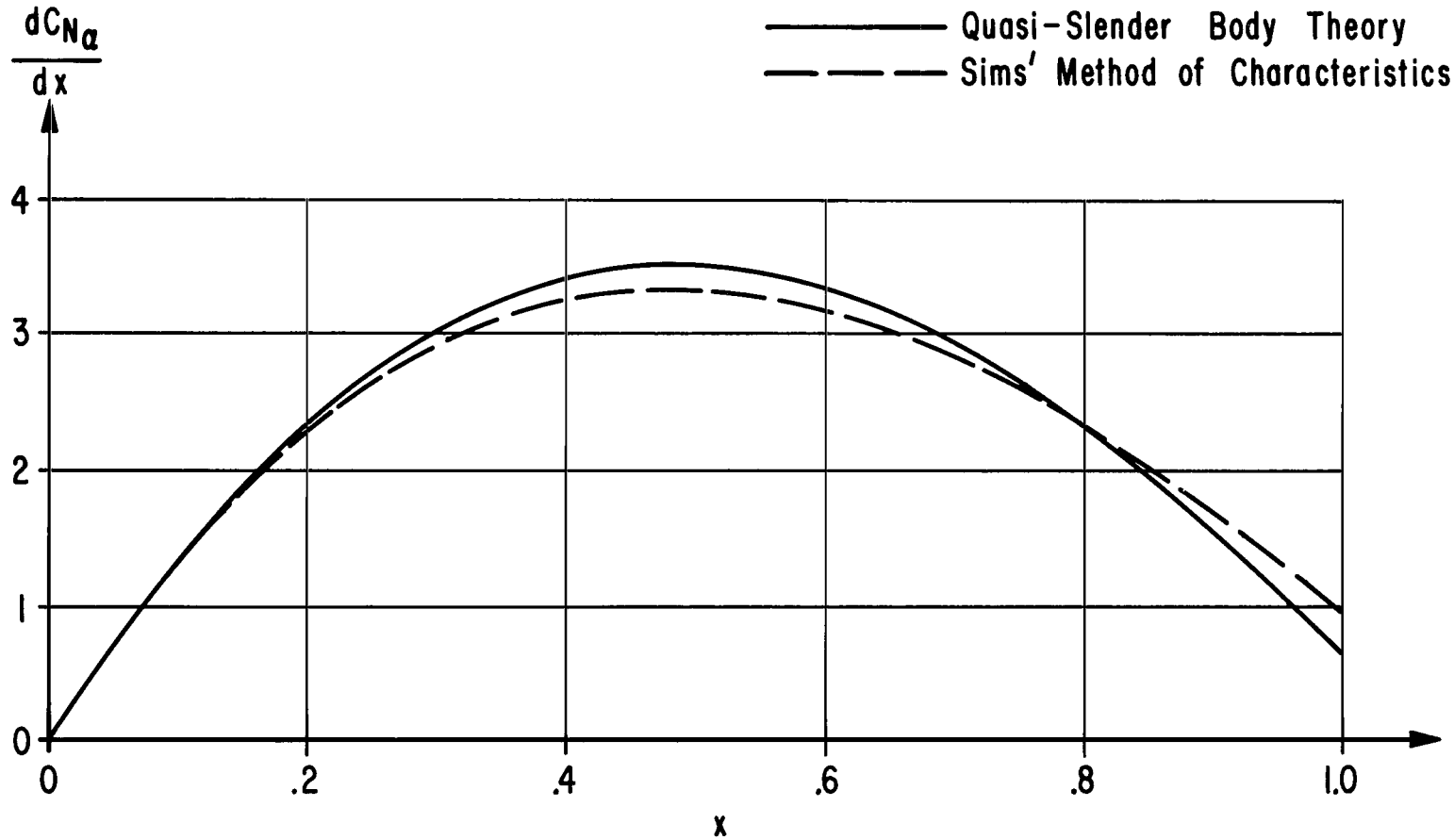

FIGURE 13. LOCAL NORMAL FORCE VARIATION FOR A CONVEX PARABOLIC OGIVE OF FINENESS RATIO 0.05 AT A MACH NUMBER OF 3.0

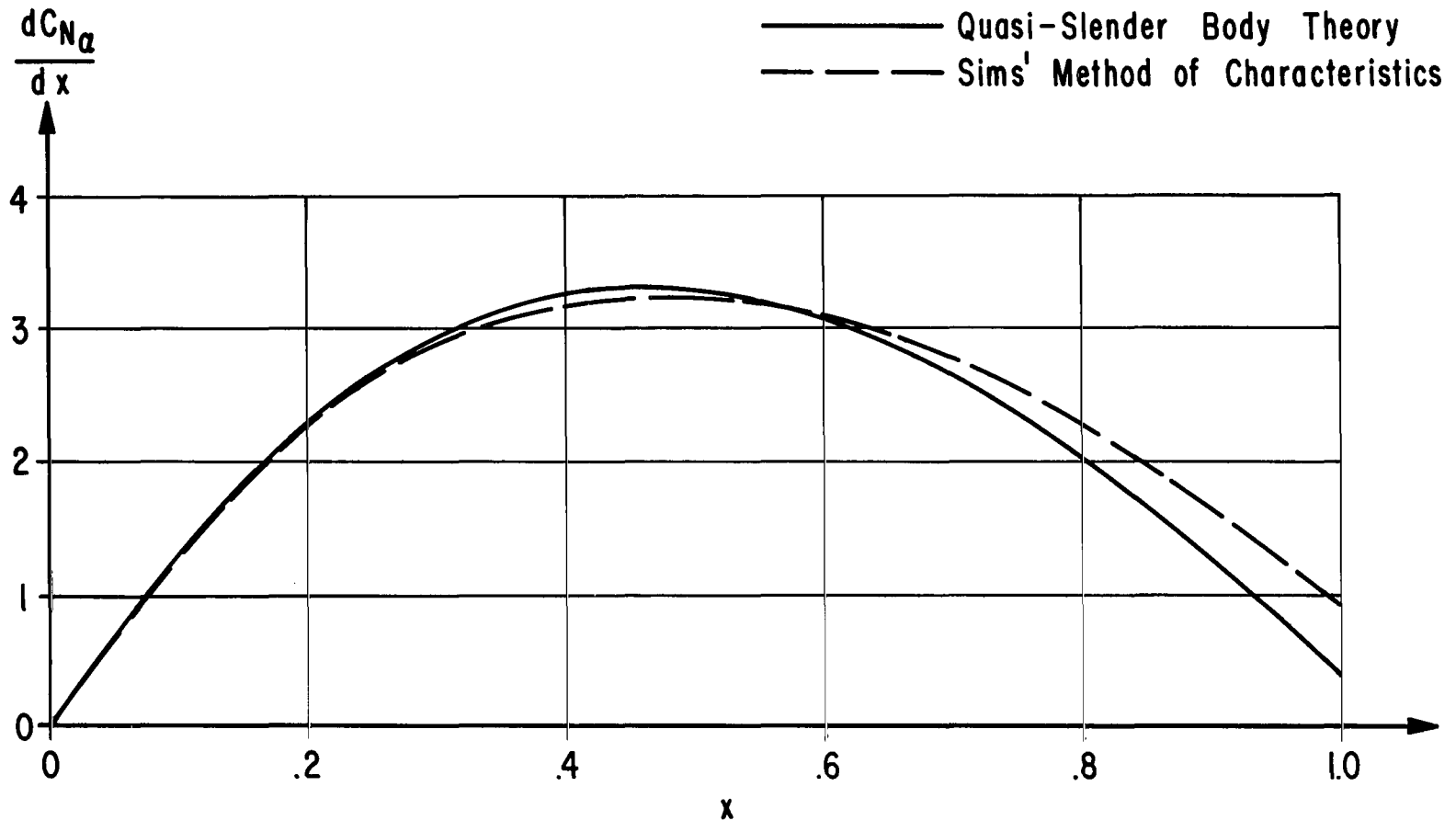

FIGURE 14. LOCAL NORMAL FORCE VARIATION FOR A CONVEX PARABOLIC OGIVE OF FINENESS RATIO 0.10 AT A MACH NUMBER OF 1.5

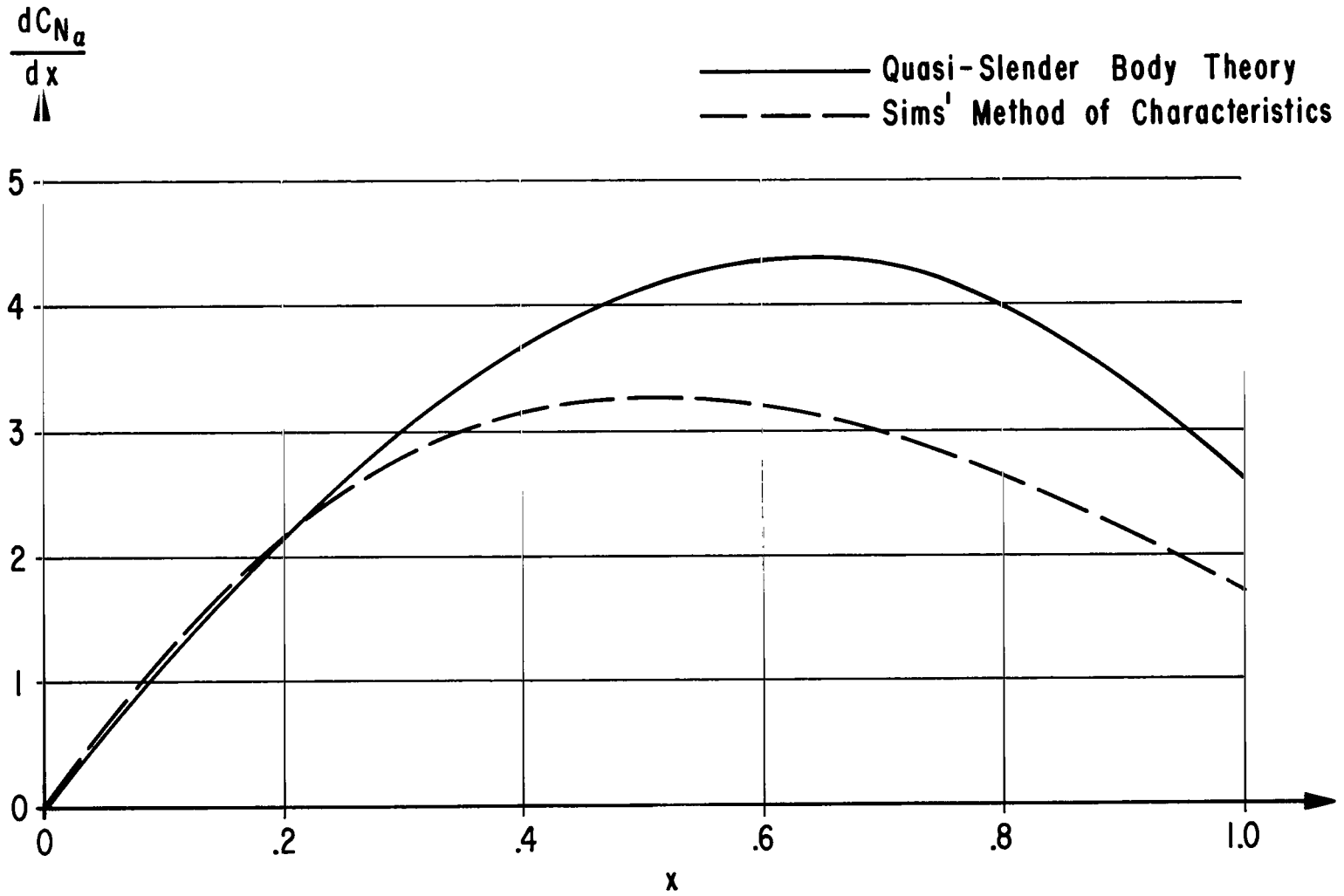

FIGURE 15. LOCAL NORMAL FORCE VARIATION FOR A CONVEX PARABOLIC OGIVE OF FINENESS RATIO 0.10 AT A MACH NUMBER OF 3.0

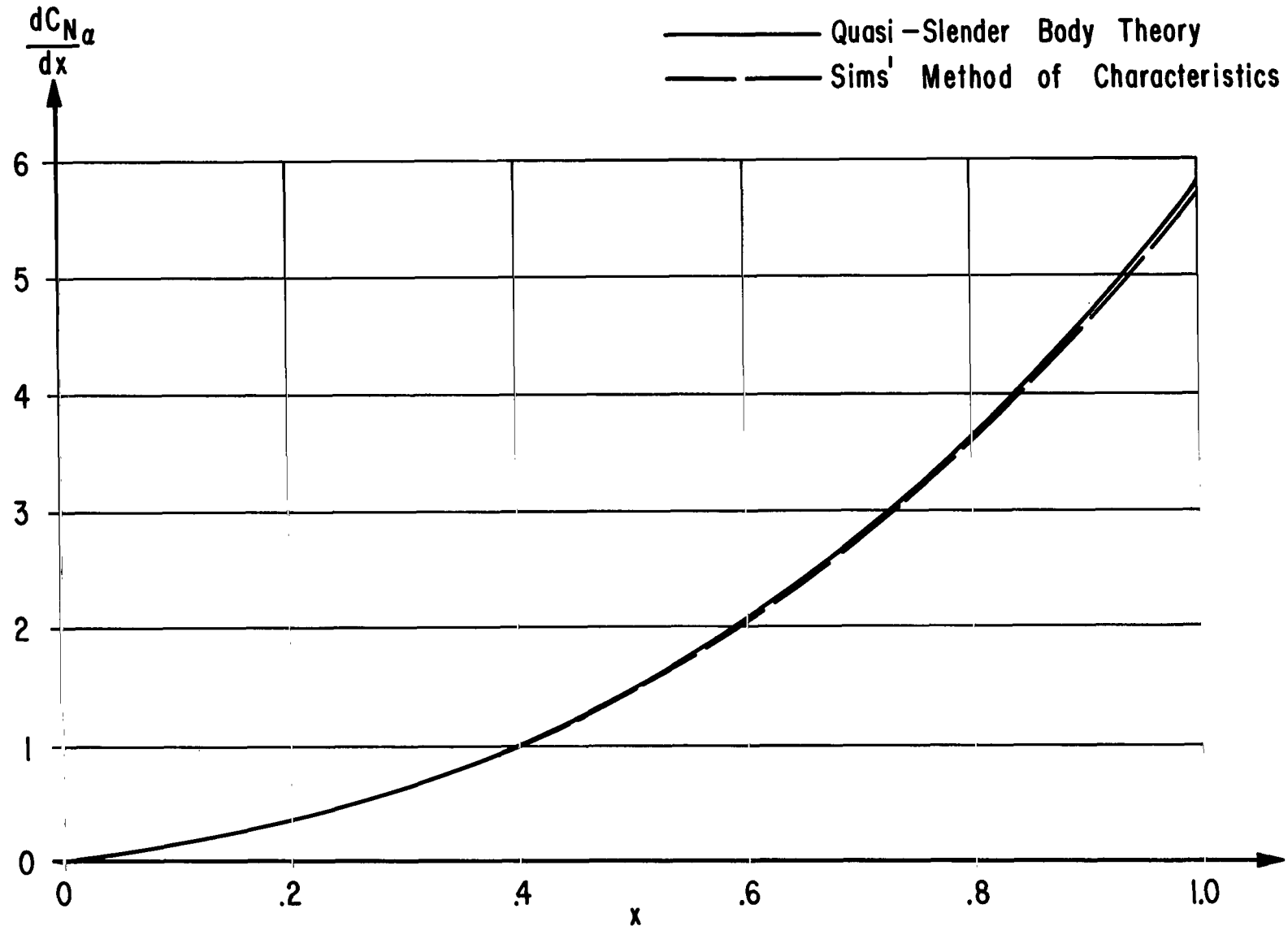

FIGURE 16. LOCAL NORMAL FORCE VARIATION FOR A CONCAVE PARABOLIC OGIVE OF FINENESS RATIO 0.05 AT A MACH NUMBER OF 1.5

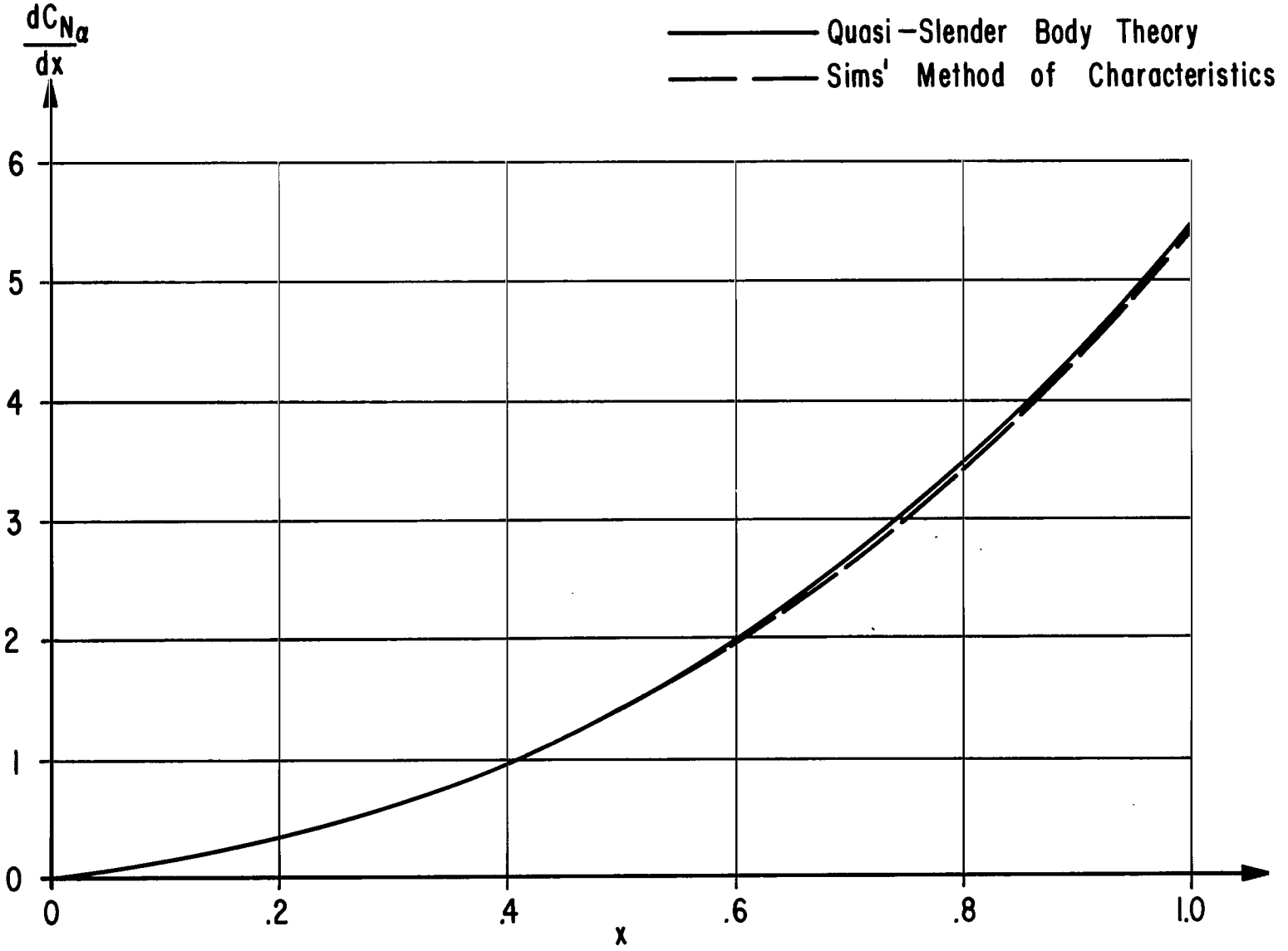

FIGURE 17. LOCAL NORMAL FORCE VARIATION FOR A CONCAVE PARABOLIC OGIVE OF FINENESS RATIO 0.05 AT A MACH NUMBER OF 3.0

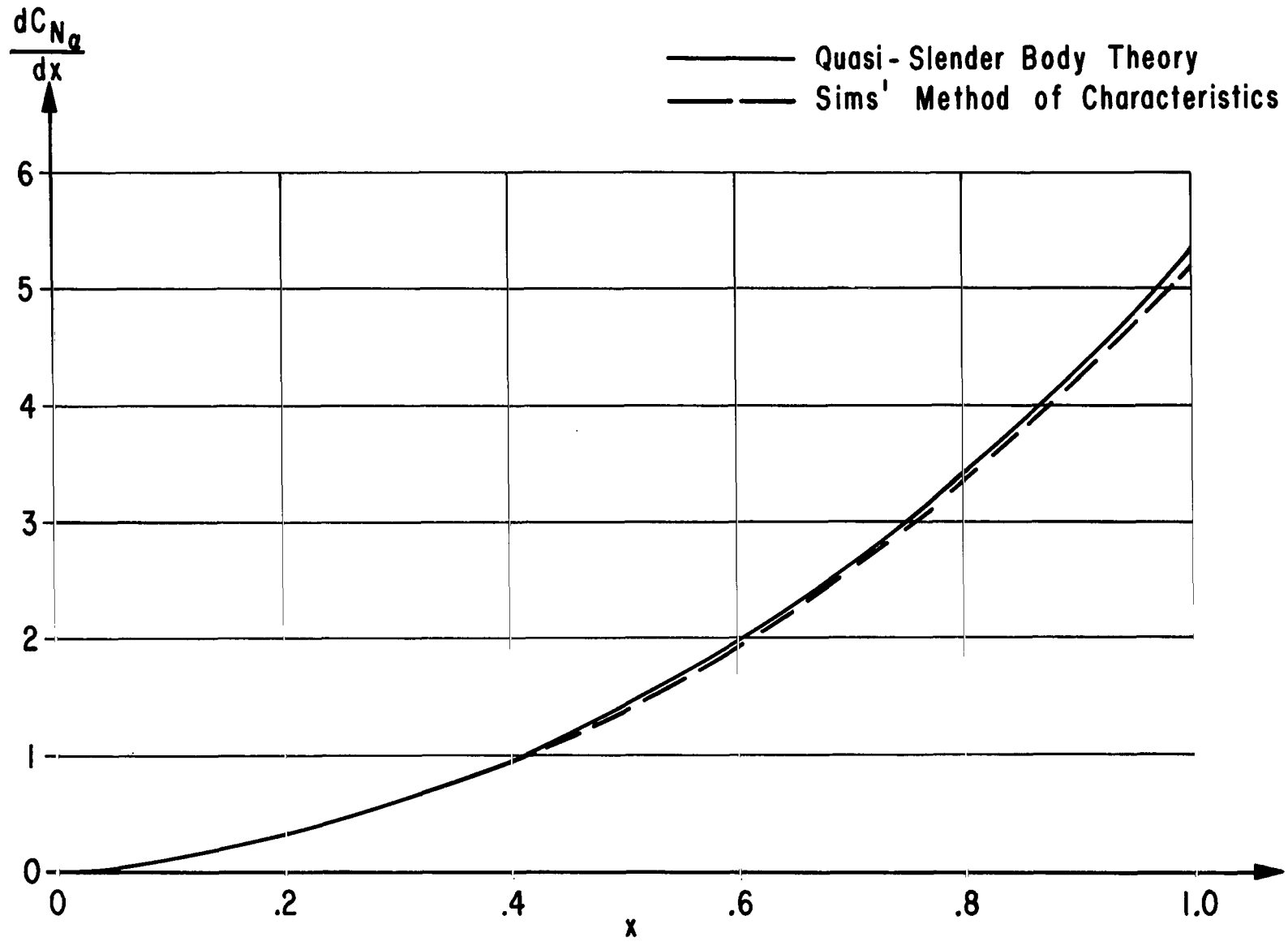

FIGURE 18. LOCAL NORMAL FORCE VARIATION FOR A CONCAVE PARABOLIC OGIVE OF FINENESS RATIO 0.10 AT A MACH NUMBER OF 1.5

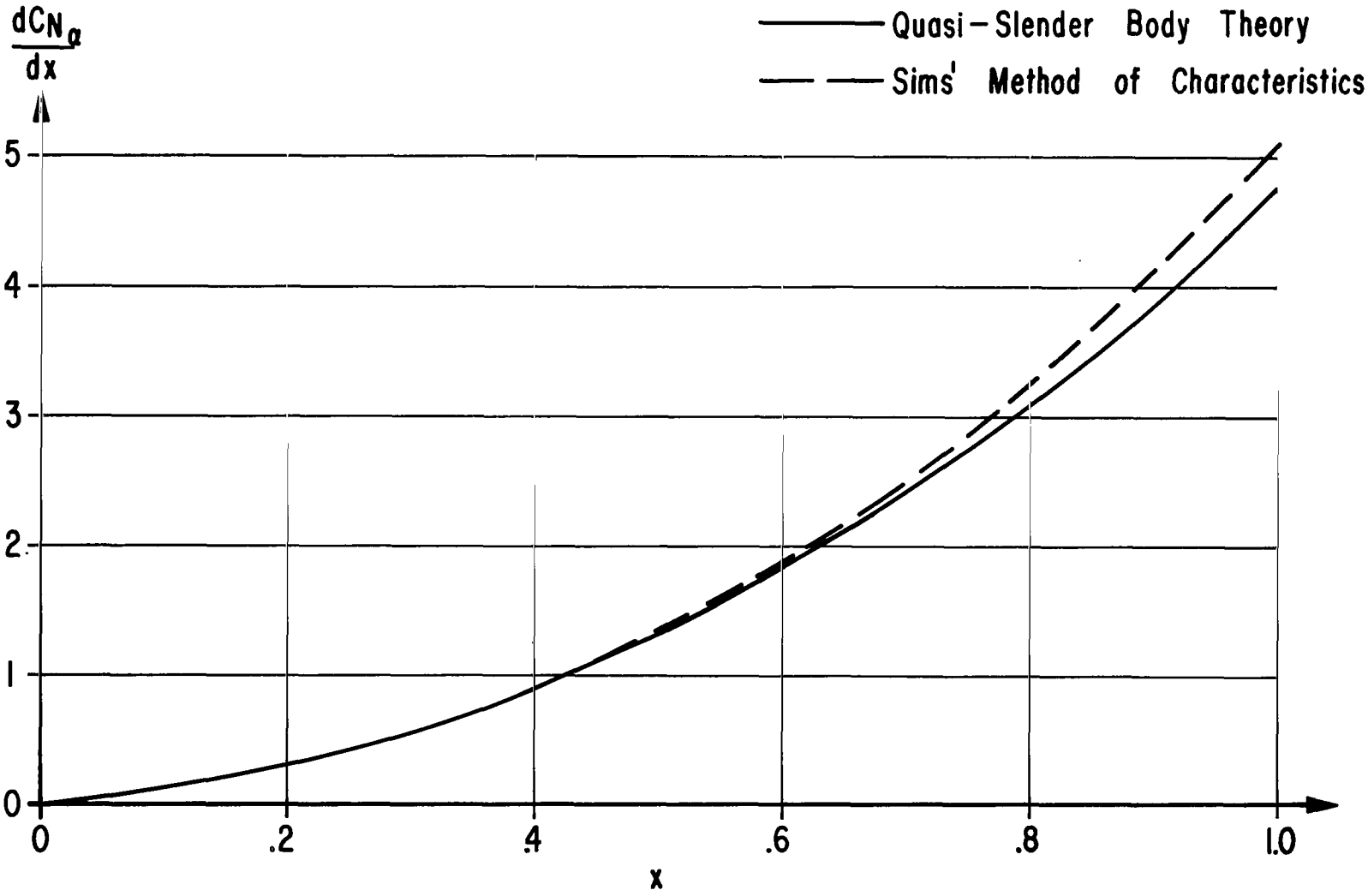

FIGURE 19. LOCAL NORMAL FORCE VARIATION FOR A CONCAVE PARABOLIC OGIVE OF FINENESS RATIO 0.10 AT A MACH NUMBER OF 3.0

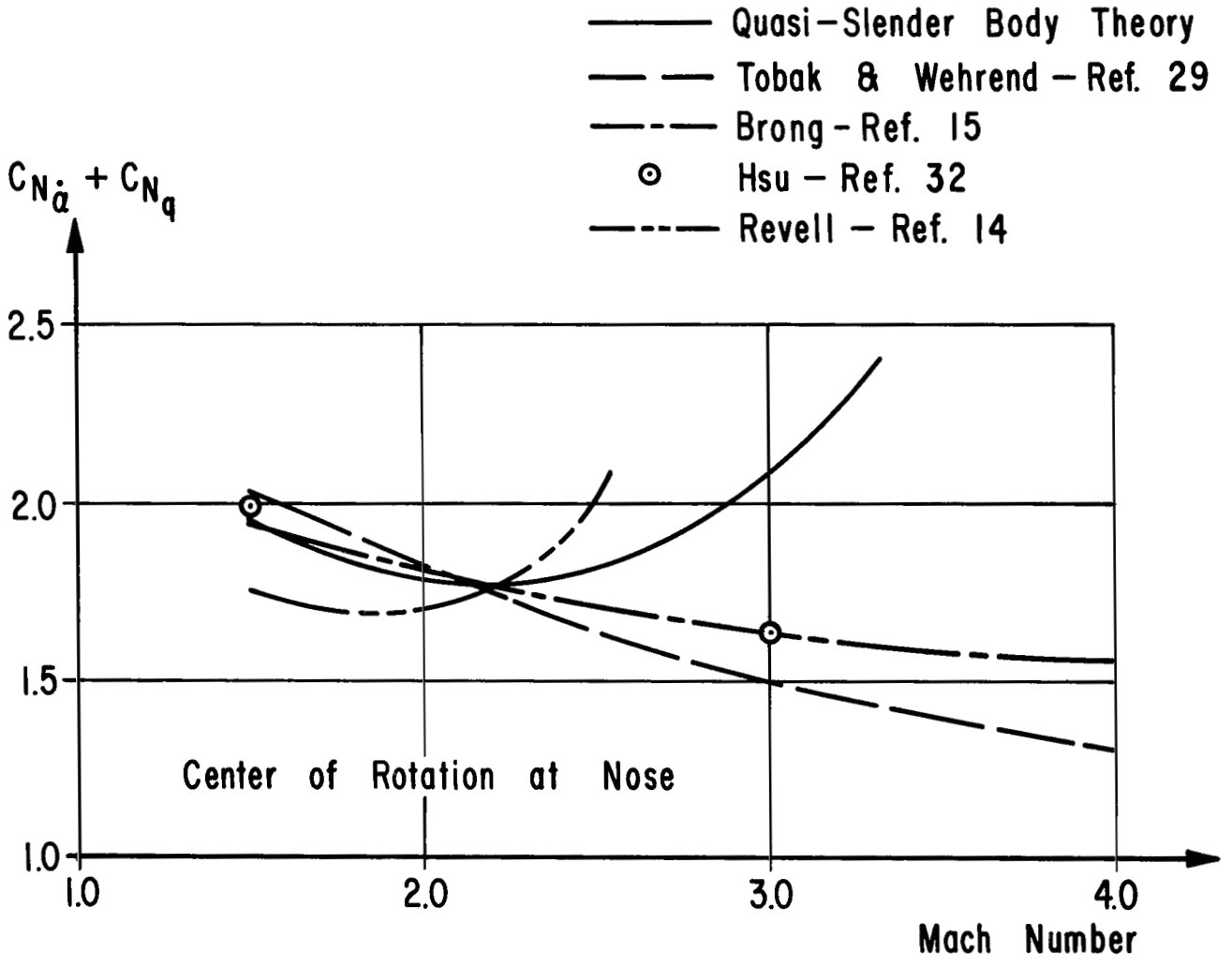

FIGURE 20. COMPARISON OF THEORETICAL RESULTS FOR FIXED AXIS DAMPING IN PITCH NORMAL FORCE COEFFICIENT FOR A 10° CONE

TABLE I

Integral	Integration Formula
$\int_0^1 x^m \ln(ax+b)\,dx$	$\frac{1}{m+1}(1-K^{m+1})\ln(a+b) + \frac{K^{m+1}}{m+1}\left(\ln b - \sum_{\nu=1}^{m+1} \frac{1}{\nu K^{\nu}}\right)$ where: $K=-\frac{b}{a}$, $a\neq 0$, $b>0$, $m\geq 0$
$\int_0^1 x^m \ln(1-x)\,dx$	$-\frac{1}{m+1}\sum_{\nu=1}^{m+1}\frac{1}{\nu}$, $m\geq 0$
$\int_0^1 x^m \ln x\,dx$	$-\left(\frac{1}{m+1}\right)^2$, $m\geq 0$
$\int_0^1\int_0^x x^m \xi^n \ln(x-\xi)\,d\xi\,dx$	$-\frac{1}{(n+1)(m+n+2)}\left[\frac{1}{m+n+2}+\sum_{\nu=1}^{n+1}\frac{1}{\nu}\right]$ $n\geq 0$, $m\geq 0$

TABLE II

$$A_m = \int_0^1 x^m \ln x \, dx$$

$$B_m = \int_0^1 x^m \ln(1-x) \, dx$$

$$C_m = \int_0^1 x^m \ln [x\,(2-x)\,] \, dx$$

$$D_m = \int_0^1 x^m \ln \left[\frac{x}{2} (1+x) \right] dx$$

$$E_{mn} = \int_0^1 \int_0^x x^m \, \xi^n \ln (x-\xi) \, d\xi \, dx$$

m	A_m	B_m	C_m	D_m
1	$-\frac{1}{4}$	-1	$2 \ln 2 - \frac{3}{2}$	$-\frac{1}{2} \ln 2$
2	$-\frac{1}{9}$	$-\frac{3}{4}$	$\frac{8}{3} \ln 2 - \frac{17}{9}$	$\frac{1}{3} \ln 2 - \frac{7}{18}$
3	$-\frac{1}{16}$	$-\frac{11}{18}$	$4 \ln 2 - \frac{67}{24}$	$-\frac{1}{4} \ln 2 + \frac{1}{12}$
4	$-\frac{1}{25}$	$-\frac{25}{48}$	$\frac{32}{5} \ln 2 - \frac{667}{150}$	$\frac{1}{5} \ln 2 - \frac{59}{300}$
5	$-\frac{1}{36}$	$-\frac{137}{300}$	$\frac{32}{3} \ln 2 - \frac{1332}{180}$	$-\frac{1}{6} \ln 2 + \frac{3}{40}$
6	$-\frac{1}{49}$	$-\frac{363}{980}$	$\frac{128}{7} \ln 2 - \frac{9319}{735}$	$\frac{1}{7} \ln 2 - \frac{379}{2940}$
7	$-\frac{1}{64}$	$-\frac{2283}{6720}$	$32 \ln 2 - \frac{74537}{3360}$	$-\frac{1}{8} \ln 2 + \frac{107}{1680}$

TABLE II (Continued)

m	E_{mn}		
	n = 0	n = 1	n = 2
1	$-\frac{4}{9}$	$-\frac{7}{32}$	$-\frac{61}{450}$
2	$-\frac{5}{16}$	$-\frac{17}{100}$	$-\frac{1}{9}$
3	$-\frac{6}{25}$	$-\frac{5}{36}$	$-\frac{83}{882}$
4	$-\frac{7}{36}$	$-\frac{23}{196}$	$-\frac{47}{576}$
5	$-\frac{8}{49}$	$-\frac{13}{128}$	$-\frac{35}{486}$

APPENDIX

Numerical Formulas for Stability Derivatives of Cones, Convex Parabolic Ogives and Concave Parabolic Ogives

Cone: $R(x) = \epsilon x$

$$C_{N_\alpha} = 2 - (2 + M^2)\,\epsilon^2 \tag{A1}$$

$$\left(C_{N_{\dot\alpha}} + C_{N_q}\right)_0 = \frac{8}{3} + \left[8\,\beta^2\left(1 - \ln\frac{2}{\beta\epsilon}\right) + 4\,M^2\left(\frac{5}{3} - \ln\frac{2}{\beta\epsilon}\right) - 4\right]\epsilon^2 \tag{A2}$$

Convex Parabolic Ogive: $R(x) = \epsilon x\,(2-x)$

$$C_{N_\alpha} = 2.0 + \left[8.0\,\beta^2 \ln\frac{2}{\beta\epsilon} - 1.3333\,M^2 + 2.6667\right]\epsilon^2 \tag{A3}$$

$$C_{M_{\alpha_0}} = -0.9333 - \left[\beta^2\left(4.1812 \ln\frac{2}{\beta\epsilon} + 2.5072\right) - 0.4190\,M^2 + 3.2762\right]\epsilon^2 \tag{A4}$$

$$\left(C_{N_{\dot\alpha}} + C_{N_q}\right)_0 = 3.0667 + \left[\beta^2\left(11.6644 \ln\frac{2}{\beta\epsilon} - 26.5163\right) - 6.3566\,M^2 - 0.3810\right]\epsilon^2 \tag{A5}$$

$$\left(C_{M_{\dot\alpha}} + C_{M_q}\right)_0 = -2.0 - \left[\beta^2\left(11.1060 \ln\frac{2}{\beta\epsilon} - 23.4400\right) + M^2\left(1.0024 \ln\frac{2}{\beta\epsilon} - 6.5391\right) + 1.8952\right]\epsilon^2 \tag{A6}$$

Concave Parabolic Ogive: $R(x) = \frac{\epsilon x}{2}(1+x)$

$$C_{N_\alpha} = 2.0 - \left[\beta^2\left(4.0 \ln \frac{2}{\beta\epsilon} - 6.1874\right) + 1.5833\, M^2 + 5.8333\right]\epsilon^2 \quad \text{(A7)}$$

$$C_{M_{\alpha_q}} = -1.4833 + \left[\beta^2\left(3.2536 \ln \frac{2}{\beta\epsilon} - 5.1211\right) + 1.2699\, M^2 - 2.9577\right]\epsilon^2 \quad \text{(A8)}$$

$$\left(C_{N_{\dot\alpha}} + C_{N_q}\right)_0 = 2.5167 - \left[\beta^2\left(16.7484 \ln \frac{2}{\beta\epsilon} - 27.8563\right) + M^2\left(5.6250 \ln \frac{2}{\beta\epsilon} - 13.0069\right) + 8.2113\right]\epsilon^2 \quad \text{(A9)}$$

$$\left(C_{M_{\dot\alpha}} + C_{M_q}\right)_0 = -2.0 + \left[\beta^2\left(14.0 \ln \frac{2}{\beta\epsilon} - 23.5935\right) + M^2\left(4.70 \ln \frac{2}{\beta\epsilon} - 10.8956\right) + 4.4155\right]\epsilon^2 \quad \text{(A10)}$$

REFERENCES

1. Munk, M. M.: The Aerodynamic Forces on Airship Hulls. NACA Rept. 184, 1923.

2. Miles, J. W.: On Non-Steady Motion of Slender Bodies. The Aeronautical Quarterly, Vol. II, Nov. 1950, pp. 183-194.

3. Dorrance, W. H.: Nonsteady Supersonic Flow About Pointed Bodies of Revolution. J. Aeron. Sci., Vol. 18, No. 8, August 1951, pp. 505-511; 542.

4. Lansing, D. L.: Velocity Potential and Forces on Oscillating Slender Bodies of Revolution in Supersonic Flow Expanded to the Fifth Power of the Frequency. NASA TN D-1225, 1962.

5. Bond, Reuben and B. B. Packard: Unsteady Aerodynamic Forces on a Slender Body of Revolution in Supersonic Flow. NASA TN D-859, 1961.

6. Landahl, M. T.: Forces and Moments on Oscillating Slender Wing-Body Combinations at Sonic Speed. AFOSR TN 56-109, M.I.T. Fluid Dynamics Research Group Report 56-1, Feb. 1956.

7. Zartarian, G. and Holt Ashley: Forces and Moments on Oscillating Slender Wing-Body Combinations at Supersonic Speed. Part I-Basic Theory. AFOSR TN 57-386, M.I.T. Fluid Dynamics Research Group Report 57-2, April 1957.

8. Platzer, M. F.: Aerodynamic Pitch Damping of Slowly Oscillating Pointed Bodies of Revolution in Linearized Supersonic Flow. NASA TMX-57417, Marshall Space Flight Center, Aug. 28, 1963.

9. Münch, J.: Calculation of Supersonic Flow Past Slowly Oscillating Bodies of Revolution by Use of Electronic Computers. AFOSR TN 57-673, Oct. 1957.

10. Bruhn, G.: Querkräfte auf langsam pendelnde schlanke Rotationskörper im Ueberschallflug. Zeitschrift für Flugwissenschaften, Vol. 9, 1961, pp. 285-299.

11. Labrujere, T. E.: Determination of the Stability Derivatives of an Oscillating Axisymmetric Fuselage in Supersonic Flow. NLL-TN W. 13, Amsterdam, 1960.

12. Holt, M.: A Linear Perturbation Method for Stability and Flutter Calculations on Hypersonic Bodies. J. Aerospace Sci., Vol. 26, No. 12, Dec. 1959, pp. 787-793.

13. Hsu, P. T. and Holt Ashley: Introductory Study of Airloads on Blunt Bodies Performing Lateral Oscillations. M. I. T. Fluid Dynamics Research Laboratory Report No. 59-9, November 1959.

14. Revell, J. D.: Second-Order Theory for Unsteady Supersonic Flow Past Slender, Pointed Bodies of Revolution. J. Aerospace Sci., Vol. 27, No. 10, Oct. 1960, pp. 739-74C.

15. Brong, E. A.: The Flow Field about a Right Circular Cone in Unsteady Flight. AIAA paper no. 65-398, presented at AIAA Second Annual Meeting, San Francisco, Calif., July 26-29, 1965.

16. Glauz, W. D.: Aerodynamic Forces on Oscillating Cones and Ogive Bodies in Supersonic Flow. Doctoral Thesis, Purdue University, January 1964.

17. von Kármán, Th. and N. B. Moore: The Resistance of Slender Bodies Moving with Supersonic Velocities with Reference to Projectiles. Trans. ASME, Vol. 54, 1932, pp. 303-310.

18. Erdmann, S. F. and K. Oswatitsch: Schnell arbeitende, lineare Charakteristiken-Verfahren für axiale und schräge Ueberschallanströmung um Rotationskörper mit Ringflächen. Zeitschrift für Flugwissenschaften, Vol. 8, 1954, pp. 201-214.

19. Lighthill, M. J.: Supersonic Flow Past Slender Pointed Bodies of Revolution at Yaw. Quart. J. Mech. Appl. Math., Vol. I, 1948, pp. 76-89.

20. Adams, M. C. and W. R. Sears: Slender-Body Theory - Review and Extension. J. Aeron. Sci., Vol. 20, No. 2, Feb. 1953, pp. 85-98.

21. Van Dyke, M. D.: First- and Second-Order Theory of Supersonic Flow Past Bodies of Revolution. J. Aeron. Sci., Vol. 18, No. 3, March 1951, pp. 161-178; 216.

22. Hoffman, G. H. and M. F. Platzer: On Supersonic Flow Past Oscillating Bodies of Revolution. AIAA Journal, Vol. 4, No. 2, Feb. 1966, pp. 370-371.

23. Heinz, C.: Ueberschallströmungen um langsam pendelnde Drehkörper. Memoires sur la Mecanique des Fluides, Publ. Scientifiques et Techniques du Ministere de l'Air, Paris, 1954, pp. 119-126.

24. Van Dyke, M. D.: Supersonic Flow Past Oscillating Airfoils Including Nonlinear Thickness Effects. NACA Report 1183, 1954.

25. Garrick, I. E.: Nonsteady Wing Characteristics, Vol. VII, High Speed Aerodynamics and Jet Propulsion, Princeton University Press 1957, pp. 668-679.

26. Miles, J. W.: On Nonsteady Flow About Pointed Bodies of Revolution. J. Aeron. Sci., Vol. 19, No. 3, March 1952, pp. 208-209.

27. Keune, F.: Reihenentwicklung des Geschwindigkeitspotentials der linearen Unter - und Ueberschallströmung für Körper nicht mehr kleiner Streckung. Zeitschrift fur Flugwissenschaften, Vol. 5, 1957, pp. 243-247.

28. Platzer, M. F.: A Note on the Solution for the Slowly Oscillating Body of Revolution in Supersonic Flow. MTP-AERO-63-28, Marshall Space Flight Center, NASA, April 23, 1963.

29. Tobak, M. and W. R. Wehrend: Stability Derivatives of Cones at Supersonic Speeds. NACA TN 3788, 1956.

30. Sims, J. L.: Unpublished results, Aero-Astrodynamics Laboratory, Marshall Space Flight Center, Huntsville, Alabama.

31. Landahl, M. T.: Unsteady Transonic Flow. Pergamon Press, New York, 1961, p. 39.

32. Hsu, P. T.: Solution of the Supersonic Flow Field Around an Oscillating Circular Cone. M.I.T. Fluid Dynamics Research Laboratory Report No. 64-5, Dec. 1964.

33. Taylor, G. I. and J. W. Maccoll: The Air Pressure on a Cone Moving at High Speed. Proc. Roy. Soc. (London) [A], Vol. 139, 1933, p. 278.

34. Sims, J. L.: Supersonic Flow around Right Circular Cones Tables for Small Angle of Attack, NASA TN D-2004.

"The aeronautical and space activities of the United States shall be conducted so as to contribute . . . to the expansion of human knowledge of phenomena in the atmosphere and space. The Administration shall provide for the widest practicable and appropriate dissemination of information concerning its activities and the results thereof."

—NATIONAL AERONAUTICS AND SPACE ACT OF 1958

NASA SCIENTIFIC AND TECHNICAL PUBLICATIONS

TECHNICAL REPORTS: Scientific and technical information considered important, complete, and a lasting contribution to existing knowledge.

TECHNICAL NOTES: Information less broad in scope but nevertheless of importance as a contribution to existing knowledge.

TECHNICAL MEMORANDUMS: Information receiving limited distribution because of preliminary data, security classification, or other reasons.

CONTRACTOR REPORTS: Technical information generated in connection with a NASA contract or grant and released under NASA auspices.

TECHNICAL TRANSLATIONS: Information published in a foreign language considered to merit NASA distribution in English.

TECHNICAL REPRINTS: Information derived from NASA activities and initially published in the form of journal articles.

SPECIAL PUBLICATIONS: Information derived from or of value to NASA activities but not necessarily reporting the results of individual NASA-programmed scientific efforts. Publications include conference proceedings, monographs, data compilations, handbooks, sourcebooks, and special bibliographies.

Details on the availability of these publications may be obtained from:

SCIENTIFIC AND TECHNICAL INFORMATION DIVISION

NATIONAL AERONAUTICS AND SPACE ADMINISTRATION

Washington, D.C. 20546